Table II. *ELISPOT assay of the anti-hNC16A IgG-producing B cells*

Mouse	Day[a]	Spleen	Lymph Node	Bone Marrow
#488	9	135 ± 16.2	43.5 ± 4.0	2 ± 0.8
#109	10	70.5 ± 5.4	84.0 ± 10.5	3.8 ± 0.6
#805	52	17.0 ± 2.7	10.5 ± 2.3	1.7 ± 0.2

$Rag\text{-}2^{-/-}/COL17^{m-/-,h+}$ mice were transferred with splenocytes of the immunized WT mice. The number of the anti-hNC16A IgG-producing B cells is displayed per 10^5 cells in spleen, lymph nodes, and bone marrow.

[a]Number of days after the transfer of immunized splenocytes.

BP model mice demonstrated a trend in which the disease severity started to decrease around 12 wk after the transfer; however, there was variation among the individual mice.

Histopathologic analysis of the lesional skin demonstrated the dermal–epidermal separation associated with mild inflammatory cell infiltration (Fig. 3H). Mast cell degranulation was observed in the dermis in toluidine blue staining (Fig. 3I). In the control $Rag\text{-}2^{-/-}$ recipients, no significant histopathologic changes were detected (Table I). Direct IF analysis of perilesional skin biopsies revealed linear deposition of IgG (Fig. 3J) and C3 (Fig. 3K) at the DEJ in all of the $Rag\text{-}2^{-/-}/COL17$–humanized recipients, whereas no IgG deposition was detected in the control $Rag\text{-}2^{-/-}$ recipients (Table I). Time-course analysis of the in situ deposition of IgG Abs in the $Rag\text{-}2^{-/-}/COL17$–humanized recipients ($n = 3$) by direct IF at days 4, 9, 14, and 21 demonstrated intense deposition of anti-hCOL17 IgG Abs at the DEJ as early as day 9 after the adoptive transfer, and the same levels of deposition were observed at days 14 and 21.

The subclasses of IgG produced in the $Rag\text{-}2^{-/-}/COL17$–humanized recipients were also analyzed by direct IF ($n = 10$). All of the $Rag\text{-}2^{-/-}/COL17$–humanized recipients showed a positive reaction with IgG1, IgG2a, IgG2b, and IgG2c Abs at the DEJ.

Immunogold electron microscopy of the perilesional skin in the $Rag\text{-}2^{-/-}/COL17$–humanized recipients showed that anti-mouse IgG Abs were located on and around the plasma membrane of the basal cells (Fig. 3L), suggesting that Abs produced in the recipients bind to hCOL17.

To further confirm the pathogenicity of IgG Abs produced in the $Rag\text{-}2^{-/-}/COL17$–humanized recipients, we purified IgG from the sera obtained from the $Rag\text{-}2^{-/-}/COL17$–humanized recipients at 8 d after the adoptive transfer and passively transferred them into COL17-humanized neonatal mice by i.p. injection. Transferred neonatal mice developed erythema around the injection site and epidermal detachment by gentle friction at 48 h after the injection (0.1, 0.5, or 1.0 mg/g body weight, $n = 5$, respectively) (Fig. 5A). Histopathologic examination of the lesional skin revealed separation between the epidermis and the dermis, with infiltration of inflammatory cells (Fig. 5B). Mast cell degranulation in the dermis was also observed in toluidine blue staining (Fig. 5C). Direct IF examinations revealed linear deposition of mouse IgG and C3 at the DEJ (Fig. 5D, 5E). In contrast, the recipient mice that received 1.0 mg/g body weight of IgG purified from WT mice showed no skin detachment, nor any histologic or immunopathologic changes ($n = 5$) (Fig. 5F–J). These findings show that IgG Abs purified from the $Rag\text{-}2^{-/-}/COL17$–humanized recipients are capable of inducing subepidermal blistering in COL17–humanized neonatal mice, which is associated with the binding of IgG Abs to the DEJ, followed by in situ activation of mouse complement and mast cell degranulation.

CD4+ T cells as well as CD45R+ B cells are essential for the stable production of anti-hCOL17 IgG Abs in the Rag-2−/−/COL17–humanized recipients

To determine the pathogenic roles of T cells and B cells in the $Rag\text{-}2^{-/-}/COL17$–humanized recipients, we depleted CD4+ or CD8+ T cells or CD45R+ B cells from splenocytes of the immunized WT
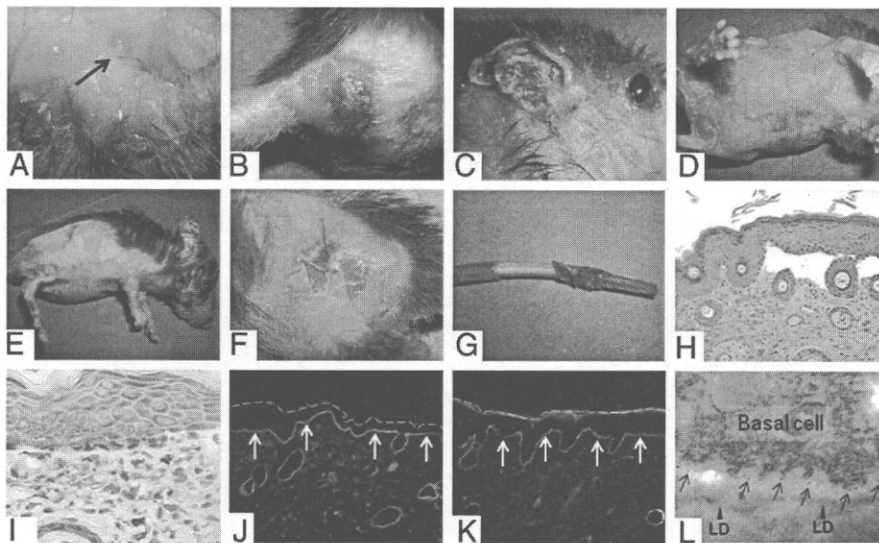
FIGURE 3. $Rag\text{-}2^{-/-}/COL17$–humanized mice given immunized splenocytes demonstrate the BP phenotype associated with histologic and immunopathologic changes similar to BP. *A*, Spontaneously developing blisters are observed in the $Rag\text{-}2^{-/-}/COL17$–humanized recipients 3 wk after the transfer (arrow). *B* and *C*, Genital erosions and ear swelling with crusts are seen in the recipients. *D* and *E*, Large, diffuse patches of hair loss associated with erythema, erosions, and crusts on the trunk and the paws. *F* and *G*, Epidermal detachment by gentle friction on the trunk and tail is characteristically observed. *H*, Histologic examination of diseased mice reveals separation between dermis and epidermis with mild inflammatory cell infiltration in H&E staining (original magnification ×200). *I*, Mast cell degranulation in the dermis is observed in toluidine blue staining (original magnification ×400). *J* and *K*, Direct IF analysis of lesional skin biopsy reveals linear deposition of mouse IgG (arrows) (*J*) and mouse C3 (arrows) (*K*) along the DEJ (original magnification ×200). *L*, Immunoelectron microscopy demonstrates that mouse IgG Abs deposit at the DEJ close to the plasma membranes of basal cells in the skin of the $Rag\text{-}2^{-/-}/COL17$–humanized recipient (arrows). LD, lamina densa.
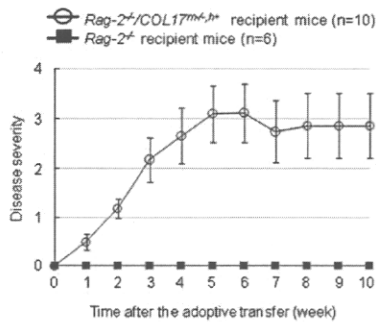
FIGURE 4. $Rag-2^{-/-}$/COL17–humanized mice given immunized splenocytes develop the BP disease phenotype. Disease severities of the Rag-$2^{-/-}$/COL17–humanized recipients gradually increase, plateauing 5 wk after the transfer. None of the control $Rag-2^{-/-}$ recipients develop any skin lesions ($n = 10$; controls, $n = 6$). Disease severity is scored as described in *Materials and Methods*.

mice and adoptively transferred them into the $Rag-2^{-/-}$/COL17–humanized mice. All of the recipient mice given immunized splenocytes after the depletion of $CD8^+$ T cells produced a high titer of anti-hCOL17 IgG Abs and developed severe BP lesions associated with histopathologic and immunopathologic changes indistinguishable from those of the $Rag-2^{-/-}$/COL17–humanized mice given whole immunized splenocytes ($n = 4$) (Fig. 6). In contrast, the depletion of $CD4^+$ T cells or $CD45R^+$ B cells inhibited the production of anti-hCOL17 IgG Abs and the development of the BP phenotype ($n = 4$, respectively) (Fig. 6). These findings indicate that $CD4^+$, but not $CD8^+$, T cells and $CD45R^+$ B cells are crucial for the production of anti-hCOL17 IgG Abs and for the development of the BP phenotype.
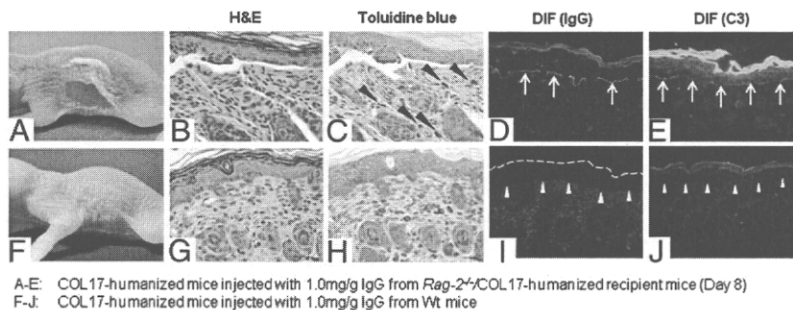
To further investigate the pathogenic role of $CD4^+$ T cells in the $Rag-2^{-/-}$/COL17–humanized recipients, we examined the efficacy of CsA (19–22). Approximately 35 mg/kg of CsA dissolved in olive oil ($n = 5$) or a control vehicle ($n = 5$) was i.p. injected into the $Rag-2^{-/-}$/COL17–humanized recipients from 2 d after the adoptive transfer of whole immunized splenocytes, once daily for 14 d. When the numbers of splenocytes at day 9 after the transfer were compared, the mean number of splenocytes in both groups was not significantly different (8.3×10^7 cells in the CsA-treated mice versus 11.0×10^7 cells in the control mice, $p > 0.05$). Although the mean percentage of $CD3^+$ T cells was significantly lower in the CsA-treated mice than that in the control mice (14.1% in the CsA-treated mice versus 24.5% in the control mice, $p <$

0.05), the mean percentages of $CD45R^+$ B cells were similar in both groups (28.8% in the CsA-treated mice versus 26.5% in the control mice, $p > 0.05$). Disease severity and the titers of circulating anti-hNC16A IgG Abs were significantly lower in the treated mice than those in the controls (Fig. 7). This result further suggests that $CD4^+$ T cells play a pivotal role in the pathogenesis of this BP model.

Discussion

This is the first active BP model that stably produces pathogenic anti-hCOL17 Abs and spontaneously develops blisters and erosions on the skin. Because amino acid sequences of COL17, especially those of the noncollagenous 16A domain region, are different between human and mouse, an animal model using COL17-humanized mice that express hCOL17 is suitable for analyzing pathogenic mechanisms of human BP. Therefore, we developed an active BP model in which the targeted pathogenic Ag is hCOL17 but not mouse COL17. Immunized splenocytes transferred into immunodeficient $Rag-2^{-/-}$/COL17–humanized recipients survived and continuously produced a high titer of anti-hCOL17 Abs in vivo for >10 wk after the adoptive transfer. Those Abs bound to the hCOL17 molecules that were expressed in the recipients' skin, which initiated subsequent immune reactions including complement activation and mast cell degranulation, resulting in dermal–epidermal separation. This array of immune responses was consistent with the pathogenic mechanisms of BP previously demonstrated in passive-transfer neonatal mouse models (1, 12, 23–25). Furthermore, the $Rag-2^{-/-}$/COL17–humanized recipients developed blisters and erosions on erythematous skin areas that lasted >10 wk. The pathogenicity of anti-hCOL17 IgG Abs was confirmed by passive-transfer experiments that revealed that IgG Abs obtained from the $Rag-2^{-/-}$/COL17–humanized recipients could induce the BP phenotype in COL17-humanized neonatal mice. Thus, pathogenic anti-hCOL17 IgG Abs produced in the $Rag-2^{-/-}$/COL17–humanized recipient binds to the target Ag in vivo and induces the BP phenotype. By using COL17-humanized mice, we can observe the dynamic immune reactions induced by pathogenic Abs against hCOL17 molecules. These strategies for the production of active autoimmune disease models targeting humanized pathogenic Ag can also be applied to other autoimmune diseases.

In BP, complement activation is considered to be critical for blister formation (26). The first evidence suggesting the pathogenic role of complements in BP is the demonstration of C3

A–E: COL17-humanized mice injected with 1.0 mg/g IgG from $Rag-2^{-/-}$/COL17-humanized recipient mice (Day 8)
F–J: COL17-humanized mice injected with 1.0 mg/g IgG from Wt mice

FIGURE 5. COL17-humanized neonatal mice injected with IgG purified from the $Rag-2^{-/-}$/COL17–humanized recipients at 8 d after the adoptive transfer show skin fragility and histologic and immunopathologic changes similar to BP. *A,* The recipient mice develop epidermal detachment by gentle friction at 48 h after injection of the 1.0 mg/g IgG purified from the $Rag-2^{-/-}$/COL17–humanized recipients ($n = 5$). *B,* Histologic examination reveals subepidermal separation associated with mild inflammatory cell infiltrates in H&E staining (original magnification ×200). *C,* Mast cell degranulation in the dermis (arrow heads) is observed in toluidine blue staining (original magnification ×400). *D* and *E,* Direct IF studies show linear deposition of mouse IgG (arrows) (*D*) and C3 (arrows) (*E*) at the DEJ (original magnification ×200). *F–J,* No phenotypic or histological findings are observed in the mice injected with 1.0 mg/g IgG purified from sera of WT mice grafted with WT skin ($n = 5$).

FIGURE 6. The production of anti-hCOL17 IgG Abs requires CD4$^+$ T cells and CD45R$^+$ B cells but not CD8$^+$ T cells. *A*, All of the recipients given CD8$^+$ T cell-depleted splenocytes ($n = 4$) develop severe BP lesions similar to those of the recipients given whole splenocytes, whereas the recipients given CD4$^+$ T cell-depleted splenocytes ($n = 4$) or CD45R$^+$ B cell-depleted splenocytes ($n = 4$) demonstrate no erosive lesions. *B*, The depletions of CD4$^+$ T cells or CD45R$^+$ B cells significantly inhibit the production of anti-hNC16A IgG Abs ($p < 0.01$ at day 9). *C*, The recipients given CD4$^+$ T cell-depleted or CD45R$^+$ B cell-depleted splenocytes show significantly lower disease severities than those in other groups ($p < 0.05$ at days 14 and 35).
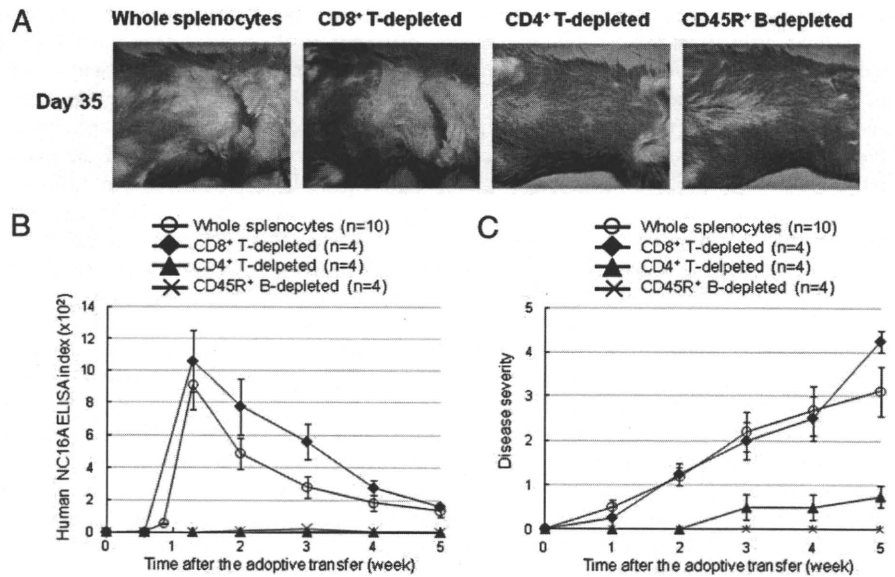
deposition at the basement membrane zone of the lesional and perilesional skin by direct IF (27). By means of the passive-transfer experiments using C5-deficient mice, Liu et al. (25) further showed that complement activation is a pivotal step in subepidermal blister formation triggered by rabbit anti-mouse COL17 IgG Abs in their BP animal model. Consistent with these previous studies, linear deposition of complement C3 was observed at the DEJ in all of the diseased *Rag-2$^{-/-}$*/COL17–humanized recipients. We also demonstrated that sera from both the immunized WT mice and the *Rag-2$^{-/-}$*/COL17–humanized recipients contained complement-fixing Abs of the IgG2 subclass and could fix compliments at the DEJ of the normal human skin and the COL17-humanized skin. Analysis of the subclass distribution of IgG autoantibodies in human BP revealed that complement-fixing IgG1 was present as the predominant subclass of autoantibodies (28). These findings suggest that complement activation mediated by Abs of the IgG2 subclass against hCOL17 may induce blister formation in the present BP model.

It is unclear why the anti-hCOL17 IgG titer decreases in a short period. To examine the possible compartmentalization of anti-hCOL17 IgG response to the skin, we checked in situ deposition of anti-hCOL17 IgG in the skin of BP model mice by direct IF analysis sequentially at days 4, 9, 14, and 21. Intense deposition of anti-hCOL17 IgG Abs was detected at the DEJ as early as day 9 of the adoptive transfer, and the same levels of deposition were observed at days 14 and 21 ($n = 3$). This indicates that the compartmentalization of the anti-hCOL17 IgG response to the skin is not the main reason for the spontaneous reduction of the anti-hCOL17 IgG titer in this BP model. Alternatively, some regulatory mechanism against hCOL17-specific T cells, B cells, or both may be induced in this BP model. In experimental autoimmune myasthenia gravis, an autoimmune neuromuscular disease model induced by anti-acetylcholine receptor Abs, regulatory T cells (Tregs) generated ex vivo or expanded in vivo suppress pathogenic T cell and Ab responses (29, 30). In experimental autoimmune encephalomyelitis, a myelin-reactive T cell-dependent multiple
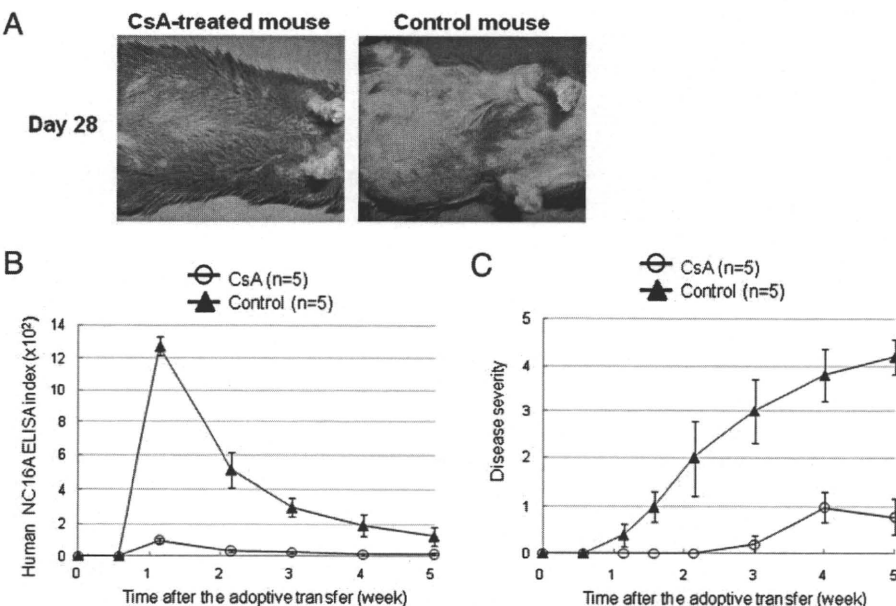
FIGURE 7. Results of CsA treatment in the *Rag-2$^{-/-}$*/COL17–humanized recipients. Approximately 35 mg/kg CsA was administered daily from 2 d after the adoptive transfer for 14 d (CsA, $n = 5$; control vehicle, $n = 5$). *A*, Skin lesions of the *Rag-2$^{-/-}$*/COL17–humanized recipients treated with CsA are markedly diminished with CsA treatment (day 28). *B*, CsA significantly suppresses the production of anti-hNC16A IgG ($p < 0.01$ at days 8, 15, and 21). *C*, The treated mice show significantly lower disease severity than that of the controls ($p < 0.01$ at days 8, 15, 21, 28, and 35).

sclerosis model, natural resolution correlates with the accumulation of myelin-reactive Tregs expanded during the course of experimental autoimmune encephalomyelitis in the inflamed CNS (31, 32). Similar to these autoimmune disease models, Tregs may contribute to the spontaneous decline of the anti-hCOL17 IgG titer in this BP model. Further studies examining Treg function in this BP model may provide clues for controlling the autoimmune reaction in BP patients.

Interestingly, none of the control $Rag-2^{-/-}$ recipients given immunized splenocytes produced anti-hCOL17 IgG Abs or developed the BP phenotype despite the presence of living splenocytes in vivo. We further demonstrated that the grafting of $hCOL17$-Tg skin onto $Rag-2^{-/-}$ mice 5 wk after the adoptive transfer of immunized splenocytes could induce a high titer of anti-hCOL17 IgG Abs. These results indicate that transferred splenocytes need endogenous hCOL17 molecules to produce anti-hCOL17 IgG Abs. In addition, the depletion of CD4$^+$ T cells from the immunized WT splenocytes suppressed the production of anti-hCOL17 IgG Abs, whereas the depletion of CD8$^+$ T cells showed no effects. This clearly suggests that CD4$^+$ T cells, and not CD8$^+$ T cells, are essential for the production of Abs against hCOL17 in this BP model.

Generally, the production of Abs by B cells requires the help of CD4$^+$ T cells. In experimental autoimmune myasthenia gravis, both MHC class II gene-disrupted mice and CD4 gene knockout mice have been proven to be resistant to induction of clinical experimental autoimmune myasthenia gravis (33, 34). In experimental pemphigus vulgaris, an autoimmune blistering disease caused by anti-desmoglein 3 Abs, the production of autoantibodies required both CD4$^+$ T cells and B cells from naive desmoglein 3 knockout mice (35). To further investigate the pathogenic role of CD4$^+$ T cells, we administered CsA, an immunosuppressant that inhibits T cell function, to the $Rag-2^{-/-}$/ COL17–humanized recipients after the adoptive transfer of immunized splenocytes. Because active disease models possess more persistent disease activity than passive-transfer neonatal disease models (10, 36, 37), we can easily analyze the time-course changes of disease activity altered by such an intervention. CsA significantly suppressed the production of anti-hNC16A IgG Abs and diminished the disease severity. These results strongly suggest that CD4$^+$ T cells play a pivotal role in the production of the autoantibodies through the presentation of the endogenous autoantigen. In human BP, the presence of autoreactive CD4$^+$ T cells has been reported, indicating the contribution of CD4$^+$ T cells to the pathogenesis of human BP (38–40). In addition, particular MHC class II alleles are more frequent in BP patients (41). These results further indicate that the autoreactive CD4$^+$ T cells may be activated through an interaction with the specific MHC class II molecule in BP. The pathogenic function of CD4$^+$ T cells shown in this BP model may provide a new insight into the pathogenic mechanism of BP and the development of a novel therapeutic strategy that targets T cell-mediated immune reactions.

Although this BP model is a useful tool for investigating the pathophysiology of BP, limitations are still present in our experimental system. First, the induction phase of the autoimmune response, such as the breakdown of self-tolerance, cannot be investigated in this BP model because the immune response to hCOL17 is induced by adoptive transfer of immunized WT splenocytes. To investigate the induction of autoimmunity in BP, Xu et al. (42) have aimed to induce autoimmune responses to mouse COL17 by using the immunocompetent BALB/c mice. Multiple immunizations of BALB/c mice with peptides of the hNC16A domain, its mouse equivalent, or both successfully induced anti-mouse COL17 IgG Abs, although no overt skin changes were observed. Similar experiments have been performed to establish an animal model for epidermolysis bullosa acquisita, a subepidermal blistering disorder

induced by Abs against type VII collagen, another hemidesmosomal protein present at the basement membrane zone (43). Anti-type VII collagen Abs and subepidermal blisters were successfully induced in the mice by repeated immunizations with recombinant mouse type VII collagen protein mixed with adjuvant, although the development of the disease phenotype depended on the strain of mice. These results indicate that repeated exposure of the self Ag in conjunction with inflammatory stimulation, such as by bacterial components, may break down peripheral tolerance and induce autoantibody production in patients with a specific genetic background. This concept is further supported by the clinical findings that BP develops preferentially in elderly people and that particular HLA class II alleles correlate with BP patients (41). Second, this BP model demonstrates immune responses against a humanized Ag of the skin; however, the response still occurs in a murine milieu. The lack of eosinophilic infiltration, a characteristic trait of human BP, in this model could be related to the difference of the effector cell function between human and mouse immune systems. Furthermore, because the MHCs in mice are different from those in humans, MHC-dependent presentation of the pathogenic Ag to the T and B cells cannot be simulated in this current BP mouse model. To overcome these issues, not only the pathogenic Ag but also the immune system should be humanized in experimental animals. Recently, quasi-human immune systems have been stably reconstituted in supra-immunodeficient NOG mice using human CD34$^+$ stem cells from various sources including bone marrow, umbilical cord blood, and peripheral blood (44, 45). This system has become a common tool for studying human immunity and diseases relating to it (46, 47). However, even in that system the development of human B cells was partially blocked, and the human T cells lost their function in the periphery (48). Further technical advances would be required to establish more accurate and reliable humanized animal models that could be used toward better understanding human diseases that involve autoimmunity.

In summary, using immunodeficient COL17-humanized mice, we have successfully developed a novel active disease model for BP that continuously produces pathogenic anti-hCOL17 IgG Abs and reproduces the BP phenotype. This study indicates that a humanized animal model is quite valuable not only for analyzing biological function of human molecules but also for investigating pathogenic mechanisms of autoimmune diseases against human proteins. This new BP model can be used for the investigation of underlying mechanisms in the development and progression of BP. Furthermore, it should facilitate the development of novel therapeutic strategies for BP.

Disclosures

The authors have no financial conflicts of interest.

References

1. Nishie, W., D. Sawamura, M. Goto, K. Ito, A. Shibaki, J. R. McMillan, K. Sakai, H. Nakamura, E. Olasz, K. B. Yancey, et al. 2007. Humanization of autoantigen. *Nat. Med.* 13: 378–383.

2. Taneja, V., and C. S. David. 2001. Lessons from animal models for human autoimmune diseases. *Nat. Immunol.* 2: 781–784.

3. Diaz, L. A., H. Ratrie, III, W. S. Saunders, S. Futamura, H. L. Squiquera, G. J. Anhalt, and G. J. Giudice. 1990. Isolation of a human epidermal cDNA corresponding to the 180-kD autoantigen recognized by bullous pemphigoid and herpes gestationis sera. Immunolocalization of this protein to the hemidesmosome. *J. Clin. Invest.* 86: 1088–1094.

4. Giudice, G. J., D. J. Emery, and L. A. Diaz. 1992. Cloning and primary structural analysis of the bullous pemphigoid autoantigen BP180. *J. Invest. Dermatol.* 99: 243–250.

5. Hopkinson, S. B., K. S. Riddelle, and J. C. Jones. 1992. Cytoplasmic domain of the 180-kD bullous pemphigoid antigen, a hemidesmosomal component: molecular and cell biologic characterization. *J. Invest. Dermatol.* 99: 264–270.

6. Bédane, C., J. R. McMillan, S. D. Balding, P. Bernard, C. Prost, J. M. Bonnetblanc, L. A. Diaz, R. A. Eady, and G. J. Giudice. 1997. Bullous pemphigoid and cicatricial pemphigoid autoantibodies react with ultrastructurally separable epitopes on the BP180 ectodomain: evidence that BP180 spans the lamina lucida. *J. Invest. Dermatol.* 108: 901–907.

7. Ishiko, A., H. Shimizu, A. Kikuchi, T. Ebihara, T. Hashimoto, and T. Nishikawa. 1993. Human autoantibodies against the 230-kD bullous pemphigoid antigen (BPAG1) bind only to the intracellular domain of the hemidesmosome, whereas those against the 180-kD bullous pemphigoid antigen (BPAG2) bind along the plasma membrane of the hemidesmosome in normal human and swine skin. *J. Clin. Invest.* 91: 1608–1615.

8. Zillikens, D., P. A. Rose, S. D. Balding, Z. Liu, M. Olague-Marchan, L. A. Diaz, and G. J. Giudice. 1997. Tight clustering of extracellular BP180 epitopes recognized by bullous pemphigoid autoantibodies. *J. Invest. Dermatol.* 109: 573–579.

9. Giudice, G. J., D. J. Emery, B. D. Zelickson, G. J. Anhalt, Z. Liu, and L. A. Diaz. 1993. Bullous pemphigoid and herpes gestationis autoantibodies recognize a common non-collagenous site on the BP180 ectodomain. *J. Immunol.* 151: 5742–5750.

10. Amagai, M., K. Tsunoda, H. Suzuki, K. Nishifuji, S. Koyasu, and T. Nishikawa. 2000. Use of autoantigen-knockout mice in developing an active autoimmune disease model for pemphigus. *J. Clin. Invest.* 105: 625–631.

11. Olasz, E. B., J. Roh, C. L. Yee, K. Arita, M. Akiyama, H. Shimizu, J. C. Vogel, and K. B. Yancey. 2007. Human bullous pemphigoid antigen 2 transgenic skin elicits specific IgG in wild-type mice. *J. Invest. Dermatol.* 127: 2807–2817.

12. Nelson, K. C., M. Zhao, P. R. Schroeder, N. Li, R. A. Wetsel, L. A. Diaz, and Z. Liu. 2006. Role of different pathways of the complement cascade in experimental bullous pemphigoid. *J. Clin. Invest.* 116: 2892–2900.

13. Nishifuji, K., M. Amagai, M. Kuwana, T. Iwasaki, and T. Nishikawa. 2000. Detection of antigen-specific B cells in patients with pemphigus vulgaris by enzyme-linked immunospot assay: requirement of T cell collaboration for autoantibody production. *J. Invest. Dermatol.* 114: 88–94.

14. Sitaru, C., S. Mihai, C. Otto, M. T. Chiriac, I. Hausser, B. Dotterweich, H. Saito, C. Rose, A. Ishiko, and D. Zillikens. 2005. Induction of dermal-epidermal separation in mice by passive transfer of antibodies specific to type VII collagen. *J. Clin. Invest.* 115: 870–878.

15. Shimizu, H., J. N. McDonald, A. R. Kennedy, and R. A. Eady. 1989. Demonstration of intra- and extracellular localization of bullous pemphigoid antigen using cryofixation and freeze substitution for postembedding immunoelectron microscopy. *Arch. Dermatol. Res.* 281: 443–448.

16. Shimizu, H., A. Ishida-Yamamoto, and R. A. Eady. 1992. The use of silver-enhanced 1-nm gold probes for light and electron microscopic localization of intra- and extracellular antigens in skin. *J. Histochem. Cytochem.* 40: 883–888.

17. Takae, Y., T. Nishikawa, and M. Amagai. 2009. Pemphigus mouse model as a tool to evaluate various immunosuppressive therapies. *Exp. Dermatol.* 18: 252–260.

18. Shibaki, A., A. Sato, J. C. Vogel, F. Miyagawa, and S. I. Katz. 2004. Induction of GVHD-like skin disease by passively transferred CD8⁺ T-cell receptor transgenic T cells into keratin 14-ovalbumin transgenic mice. *J. Invest. Dermatol.* 123: 109–115.

19. Bianchi, L., S. Gatti, and G. Nini. 1992. Bullous pemphigoid and severe erythrodermic psoriasis: combined low-dose treatment with cyclosporine and systemic steroids. *J. Am. Acad. Dermatol.* 27: 278.

20. Curley, R. K., and C. A. Holden. 1991. Steroid-resistant bullous pemphigoid treated with cyclosporin A. *Clin. Exp. Dermatol.* 16: 68–69.

21. Thivolet, J., H. Barthelemy, G. Rigot-Muller, and A. Bendelac. 1985. Effects of cyclosporin on bullous pemphigoid and pemphigus. *Lancet* 325: 334–335.

22. Barthélémy, H., J. Thivolet, F. Cambazard, A. Bendelac, G. Mauduit, F. Granier, and A. Frappaz. 1986. [Cyclosporin in the treatment of bullous pemphigoid: preliminary study]. *Ann. Dermatol. Venereol.* 113: 309–313.

23. Chen, R., G. Ning, M. L. Zhao, M. G. Fleming, L. A. Diaz, Z. Werb, and Z. Liu. 2001. Mast cells play a key role in neutrophil recruitment in experimental bullous pemphigoid. *J. Clin. Invest.* 108: 1151–1158.

24. Liu, Z., L. A. Diaz, J. L. Troy, A. F. Taylor, D. J. Emery, J. A. Fairley, and G. J. Giudice. 1993. A passive transfer model of the organ-specific autoimmune disease, bullous pemphigoid, using antibodies generated against the hemidesmosomal antigen BP180. *J. Clin. Invest.* 92: 2480–2488.

25. Liu, Z., G. J. Giudice, S. J. Swartz, J. A. Fairley, G. O. Till, J. L. Troy, and L. A. Diaz. 1995. The role of complement in experimental bullous pemphigoid. *J. Clin. Invest.* 95: 1539–1544.

26. Jordon, R. E., S. Kawana, and K. A. Fritz. 1985. Immunopathologic mechanisms in pemphigus and bullous pemphigoid. *J. Invest. Dermatol.* 85: 72s–78s.

27. Provost, T. T., and T. B. Tomasi, Jr. 1973. Evidence for complement activation via the alternate pathway in skin diseases, I. Herpes gestationis, systemic lupus erythematosus, and bullous pemphigoid. *J. Clin. Invest.* 52: 1779–1787.

28. Sitaru, C., S. Mihai, and D. Zillikens. 2007. The relevance of the IgG subclass of autoantibodies for blister induction in autoimmune bullous skin diseases. *Arch. Dermatol. Res.* 299: 1–8.

29. Aricha, R., T. Feferman, S. Fuchs, and M. C. Souroujon. 2008. Ex vivo generated regulatory T cells modulate experimental autoimmune myasthenia gravis. *J. Immunol.* 180: 2132–2139.

30. Sheng, J. R., L. Li, B. B. Ganesh, C. Vasu, B. S. Prabhakar, and M. N. Meriggioli. 2006. Suppression of experimental autoimmune myasthenia gravis by granulocyte-macrophage colony-stimulating factor is associated with an expansion of FoxP3⁺ regulatory T cells. *J. Immunol.* 177: 5296–5306.

31. McGeachy, M. J., L. A. Stephens, and S. M. Anderton. 2005. Natural recovery and protection from autoimmune encephalomyelitis: contribution of CD4⁺CD25⁺ regulatory cells within the central nervous system. *J. Immunol.* 175: 3025–3032.

32. O'Connor, R. A., K. H. Malpass, and S. M. Anderton. 2007. The inflamed central nervous system drives the activation and rapid proliferation of Foxp3⁺ regulatory T cells. *J. Immunol.* 179: 958–966.

33. Kaul, R., M. Shenoy, E. Goluszko, and P. Christadoss. 1994. Major histocompatibility complex class II gene disruption prevents experimental autoimmune myasthenia gravis. *J. Immunol.* 152: 3152–3157.

34. Zhang, G. X., B. G. Xiao, M. Bakhiet, P. van der Meide, H. Wigzell, H. Link, and T. Olsson. 1996. Both CD4⁺ and CD8⁺ T cells are essential to induce experimental autoimmune myasthenia gravis. *J. Exp. Med.* 184: 349–356.

35. Aoki-Ota, M., K. Tsunoda, T. Ota, T. Iwasaki, S. Koyasu, M. Amagai, and T. Nishikawa. 2004. A mouse model of pemphigus vulgaris by adoptive transfer of naive splenocytes from desmoglein 3 knockout mice. *Br. J. Dermatol.* 151: 346–354.

36. Christadoss, P., M. Poussin, and C. Deng. 2000. Animal models of myasthenia gravis. *Clin. Immunol.* 94: 75–87.

37. Mendel, I., N. Kerlero de Rosbo, and A. Ben-Nun. 1995. A myelin oligodendrocyte glycoprotein peptide induces typical chronic experimental autoimmune encephalomyelitis in H-2ᵇ mice: fine specificity and T cell receptor Vβ expression of encephalitogenic T cells. *Eur. J. Immunol.* 25: 1951–1959.

38. Büdinger, L., L. Borradori, C. Yee, R. Eming, S. Ferencik, H. Grosse-Wilde, H. F. Merk, K. Yancey, and M. Hertl. 1998. Identification and characterization of autoreactive T cell responses to bullous pemphigoid antigen 2 in patients and healthy controls. *J. Clin. Invest.* 102: 2082–2089.

39. Lin, M. S., C. L. Fu, G. J. Giudice, M. Olague-Marchan, A. M. Lazaro, P. Stastny, and L. A. Diaz. 2000. Epitopes targeted by bullous pemphigoid T lymphocytes and autoantibodies map to the same sites on the bullous pemphigoid 180 ectodomain. *J. Invest. Dermatol.* 115: 955–961.

40. Thoma-Uszynski, S., W. Uter, S. Schwietzke, G. Schuler, L. Borradori, and M. Hertl. 2006. Autoreactive T and B cells from bullous pemphigoid (BP) patients recognize epitopes clustered in distinct regions of BP180 and BP230. *J. Immunol.* 176: 2015–2023.

41. Delgado, J. C., D. Turbay, E. J. Yunis, J. J. Yunis, E. D. Morton, K. Bhol, R. Norman, C. A. Alper, R. A. Good, and R. Ahmed. 1996. A common major histocompatibility complex class II allele HLA-DQB1* 0301 is present in clinical variants of pemphigoid. *Proc. Natl. Acad. Sci. USA* 93: 8569–8571.

42. Xu, L., N. Robinson, S. D. Miller, and L. S. Chan. 2001. Characterization of BALB/c mice B lymphocyte autoimmune responses to skin basement membrane component type XVII collagen, the target antigen of autoimmune skin disease bullous pemphigoid. *Immunol. Lett.* 77: 105–111.

43. Sitaru, C., M. T. Chiriac, S. Mihai, J. Büning, A. Gebert, A. Ishiko, and D. Zillikens. 2006. Induction of complement-fixing autoantibodies against type VII collagen results in subepidermal blistering in mice. *J. Immunol.* 177: 3461–3468.

44. Ishikawa, F., M. Yasukawa, B. Lyons, S. Yoshida, T. Miyamoto, G. Yoshimoto, T. Watanabe, K. Akashi, L. D. Shultz, and M. Harada. 2005. Development of functional human blood and immune systems in NOD/SCID/IL2 receptor γ chainⁿᵘˡˡ mice. *Blood* 106: 1565–1573.

45. Ito, M., H. Hiramatsu, K. Kobayashi, K. Suzue, M. Kawahata, K. Hioki, Y. Ueyama, Y. Koyanagi, K. Sugamura, K. Tsuji, et al. 2002. NOD/SCID/γcⁿᵘˡˡ mouse: an excellent recipient mouse model for engraftment of human cells. *Blood* 100: 3175–3182.

46. Kumar, P., H. S. Ban, S. S. Kim, H. Wu, T. Pearson, D. L. Greiner, A. Laouar, J. Yao, V. Haridas, K. Habiro, et al. 2008. T cell-specific siRNA delivery suppresses HIV-1 infection in humanized mice. *Cell* 134: 577–586.

47. Yajima, M., K. Imadome, A. Nakagawa, S. Watanabe, K. Terashima, H. Nakamura, M. Ito, N. Shimizu, M. Honda, N. Yamamoto, and S. Fujiwara. 2008. A new humanized mouse model of Epstein-Barr virus infection that reproduces persistent infection, lymphoproliferative disorder, and cell-mediated and humoral immune responses. *J. Infect. Dis.* 198: 673–682.

48. Watanabe, Y., T. Takahashi, A. Okajima, M. Shiokawa, N. Ishii, I. Katano, R. Ito, M. Ito, M. Minegishi, N. Minegishi, et al. 2009. The analysis of the functions of human B and T cells in humanized NOD/shi-scid/γcⁿᵘˡˡ (NOG) mice (hu-HSC NOG mice). *Int. Immunol.* 21: 843–858.

Successful Treatment of Nail Lichen Planus with Topical Tacrolimus

Hideyuki Ujiie, Akihiko Shibaki, Masashi Akiyama and Hiroshi Shimizu

Department of Dermatology, Hokkaido University Graduate School of Medicine, North 15 West 7, Kita-ku, Sapporo 060-8638, Japan. E-mail: h-ujiie@ med.hokudai.ac.jp

Sir,

Nail lichen planus (NLP) is characterized by thinning, longitudinal ridging and distal splitting of the nail plate (1, 2). Although mild NLP is usually asymptomatic, deformation of the fingernails is cosmetically distressing. Failure to treat NLP results in nail loss or permanent nail dystrophy in some cases. Therefore the condition should be treated effectively in its early stage. NLP is usually resistant to topical corticosteroid therapy, but successful treatment has been reported with intralesional or systemic administration of corticosteroids (2–4). However, some patients are unable to tolerate the side-effects of systemic corticosteroids.

Topical tacrolimus has been reported as a safe, effective therapy for cutaneous (5, 6), oral (7–9) and vulvar lichen planus (LP) (9–11), even in patients whose lesions have shown recalcitrance to other treatments (7, 10). However, topical tacrolimus treatment for NLP has never been reported. We report here five cases of NLP treated successfully with tacrolimus ointment.

CASE REPORTS

Five Japanese patients with NLP were treated with 0.1% tacrolimus ointment. The mean age of the five patients (4 males and 1 female) was 40.2 years (age range 11–58 years). All of the patients were diagnosed with NLP on the basis of clinical history, typical clinical appearance and histopathological features. No patient had any symptoms suggesting lupus erythematosus or photosensitivity. There was no history of nail matrix trauma, or drug intake that could cause lichenoid drug eruption. All of these cases demonstrated multiple nail lesions on the fingers and/ or toes. In one patient, the disease affected all 20 nails. All the fingernails were affected in three other patients, including two cases that presented with additional nail lesions on both big toes. The most common clinical signs were thinning of nails and onycholysis, which were observed in all of the patients. Longitudinal ridging and onychorrhexis were present in four cases. The NLP was not associated with any objective symptom, such as burning, itching or pain, in any of the cases. A 58-year-old patient had concomitant localized reticular oral LP, although no patient had cutaneous, otic or genital lesions at any time during the follow-up. An 11-year-old patient had mild atopic dermatitis; the four adult patients had no other dermatological conditions. The clinical diagnosis was confirmed by histopathological examination in all cases. Biopsy specimens taken from the affected nail matrix demonstrated band-like lymphocyte infiltration in the nail matrix and the nail bed dermis, as well as hyperkeratosis, acanthosis and hypergranulosis of the epidermis, which are histopathological features typically observed in NLP.

The mean duration of the disease prior to the topical tacrolimus treatment was 24 months (range 4–84 months). We followed up all the patients for at least 15 months (mean 39.0 months; range 15–71 months). Four of the patients had been treated with topical corticosteroids, with no or slight improvement, before the tacrolimus therapy. In all the cases, 0.1% topical tacrolimus (Protopic ointment 0.1%, Astellas Pharma Inc., Tokyo, Japan) was administered twice a day on one side of the nail plates and periungual regions of the fingers and/or toes, and a topical corticosteroid (from the classification "very strong" or "strongest") was simultaneously started on the other side for a comparison of relative efficacy. In all cases, the affected nails treated with topical tacrolimus began to improve within 6 months after the initiation of treatment (mean 2.8 months; range 1–6 months), whereas no obvious changes, or only slight improvement, were observed in the nails treated with topical corticosteroids, suggesting that tacrolimus ointment had higher therapeutic efficacy than topical corticosteroids (Fig. 1). All the lesions were then treated uniformly with topical tacrolimus. All of the patients showed marked improvement (Fig. 2). Mild onycholysis and splitting of the nails remained in some of the patients. Reticular oral LP observed in a 58-year-old patient remained after his NLP lesions had improved. Two patients who discontinued topical tacrolimus application showed no exacerbation of their lesions at 16 and 36 months of follow-up, respectively. Two other patients continue to use topical tacrolimus once or twice daily as a supportive treatment, which keeps their lesions stable. The remaining patient stopped visiting our clinic after remission. No adverse effects were noted in any of the cases.

DISCUSSION

Topical corticosteroid therapy is commonly considered as a first-line treatment for NLP, although it is usually ineffective. Oral prednisone and intramuscular triamcinolone acetonide have been reported as effective against NLP (2–4), but prolonged or repeated use of
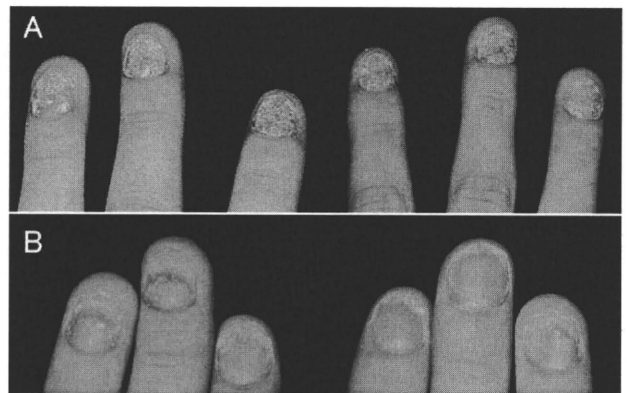

Fig. 1. (A) Nail lichen planus in an 11-year-old male patient before treatment. The fingernails show very severe thinning. The right-hand fingernails were treated with topical tacrolimus and the left-hand ones with diflucortolone valerate ointment twice daily (comparative application). (B) The same patient after 5 months of comparative application. Significant clinical improvement of the right-hand fingernails (*right*) was noted compared with the left-hand ones (*left*).
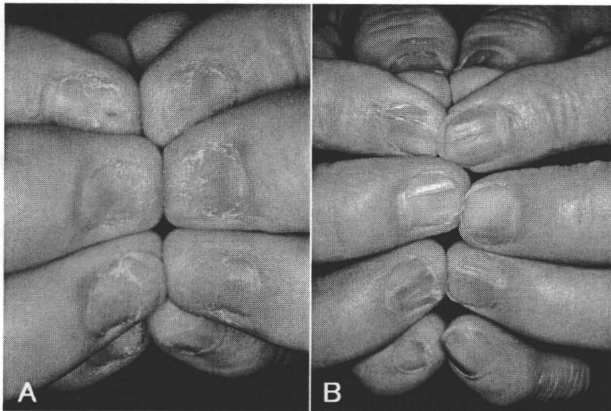
Fig. 2. (A) Nail lichen planus in a 58-year-old male patient. The fingernails show severe distal thinning and onycholysis before treatment. (B) Significant improvement after 18 months of topical tacrolimus treatment.

systemic corticosteroids may cause considerable side-effects.

Tacrolimus is a macrolide immune modulator that produces strong immunosuppression by inhibiting T-cell activation. It interacts with a cyclophilin-like cytoplasmic protein, FK506 binding protein, and this complex interferes with the phosphatase activity of calcineurin, resulting in the inhibition of proinflammatory cytokine genes transcription. Because activated T cells are likely to play a central role in the pathogenesis of LP (1, 12, 13), topical tacrolimus has been tried for the treatment of LP. Previous studies have reported that topical tacrolimus is effective for 88–100% of cases of oral LP (7–9) and 94% of cases of vulvar LP (10). Based on these data, we speculated that topical tacrolimus could also be effective against NLP. In this study, all five cases with NLP responded fairly well to topical tacrolimus, even though 4 had intractable lesions that had shown resistance to topical corticosteroids. Comparative study of the efficacy of topical tacrolimus and topical corticosteroids revealed that topical tacrolimus was more effective than topical corticosteroids in all of the cases.

Recent studies demonstrated that nail dystrophy associated with chronic paronychia (14) and eczema (15) improved with topical tacrolimus, which suggests that topical tacrolimus could penetrate the periungual skin enough to improve the nail dystrophy. In addition, the remarkable thinning of the nails and onychorrhexis seen in most of our NLP cases make it possible that the tacrolimus ointment penetrated the damaged nail plates.

The majority of oral LP and vulvar LP cases respond to topical tacrolimus within one month (7–11), whereas the present NLP patients required several months to start to regress (mean 2.8 months).

At present, two out of the five patients have been continuing once- or twice-daily application for 35 and 63 months, respectively, to keep their lesions under con-

trol. Two other patients have been stable without topical tacrolimus for more than one year. However, we should be aware of the possibility that NLP can recur, because previous reports have mentioned that oral or vulvar LP lesions usually returned after withdrawal of topical tacrolimus (7, 10). Further analysis with longer follow-up is required to confirm the long-term prognosis of NLP after the cessation of topical tacrolimus therapy.

The authors declare no conflict of interest.

REFERENCES

1. Boyd AS, Neldner KH. Lichen planus. J Am Acad Dermatol 1991; 25: 593–619.
2. Tosti A, Peluso AM, Fanti PA, Piraccini BM. Nail lichen planus: clinical and pathologic study of twenty-four patients. J Am Acad Dermatol 1993; 28: 724–730.
3. Evans AV, Roest MA, Fletcher CL, Lister R, Hay RJ. Isolated lichen planus of the toe nails treated with oral prednisolone. Clin Exp Dermatol 2001; 26: 412–414.
4. Tosti A, Piraccini BM, Cambiaghi S, Jorizzo M. Nail lichen planus in children: clinical features, response to treatment, and long-term follow-up. Arch Dermatol 2001; 137: 1027–1032.
5. Al-Khenaizan S, Al Mubarak L. Ulcerative lichen planus of the sole: excellent response to topical tacrolimus. Int J Dermatol 2008; 47: 626–628.
6. Fortina AB, Giulioni E, Tonin E. Topical tacrolimus in the treatment of lichen planus in a child. Pediatr Dermatol 2008; 25: 570–571.
7. Byrd JA, Davis MD, Bruce AJ, Drage LA, Rogers RS, 3rd. Response of oral lichen planus to topical tacrolimus in 37 patients. Arch Dermatol 2004; 140: 1508–1512.
8. Olivier V, Lacour JP, Mousnier A, Garraffo R, Monteil RA, Ortonne JP. Treatment of chronic erosive oral lichen planus with low concentrations of topical tacrolimus: an open prospective study. Arch Dermatol 2002; 138: 1335–1338.
9. Vente C, Reich K, Rupprecht R, Neumann C. Erosive mucosal lichen planus: response to topical treatment with tacrolimus. Br J Dermatol 1999; 140: 338–342.
10. Byrd JA, Davis MD, Rogers RS, 3rd. Recalcitrant symptomatic vulvar lichen planus: response to topical tacrolimus. Arch Dermatol 2004; 140: 715–720.
11. Kirtschig G, Van Der Meulen AJ, Ion Lipan JW, Stoof TJ. Successful treatment of erosive vulvovaginal lichen planus with topical tacrolimus. Br J Dermatol 2002; 147: 625–626.
12. Shiohara T, Moriya N, Nagashima M. The lichenoid tissue reaction. A new concept of pathogenesis. Int J Dermatol 1988; 27: 365–374.
13. Shiohara T, Nickoloff BJ, Moriya N, Gotoh C, Nagashima M. In vivo effects of interferon-gamma and anti-interferon-gamma antibody on the experimentally induced lichenoid tissue reaction. Br J Dermatol 1988; 119: 199–206.
14. Rigopoulos D, Gregoriou S, Belyayeva E, Larios G, Kontochristopoulos G, Katsambas A. Efficacy and safety of tacrolimus ointment 0.1% vs. betamethasone 17-valerate 0.1% in the treatment of chronic paronychia: an unblinded randomized study. Br J Dermatol 2009; 160: 858–860.
15. Lee DY, Kim WS, Lee KJ, Kim JA, Park JH, Cho HJ, et al. Tacrolimus ointment in onychodystrophy associated with eczema. J Eur Acad Dermatol Venereol 2007; 21: 1137–1138.
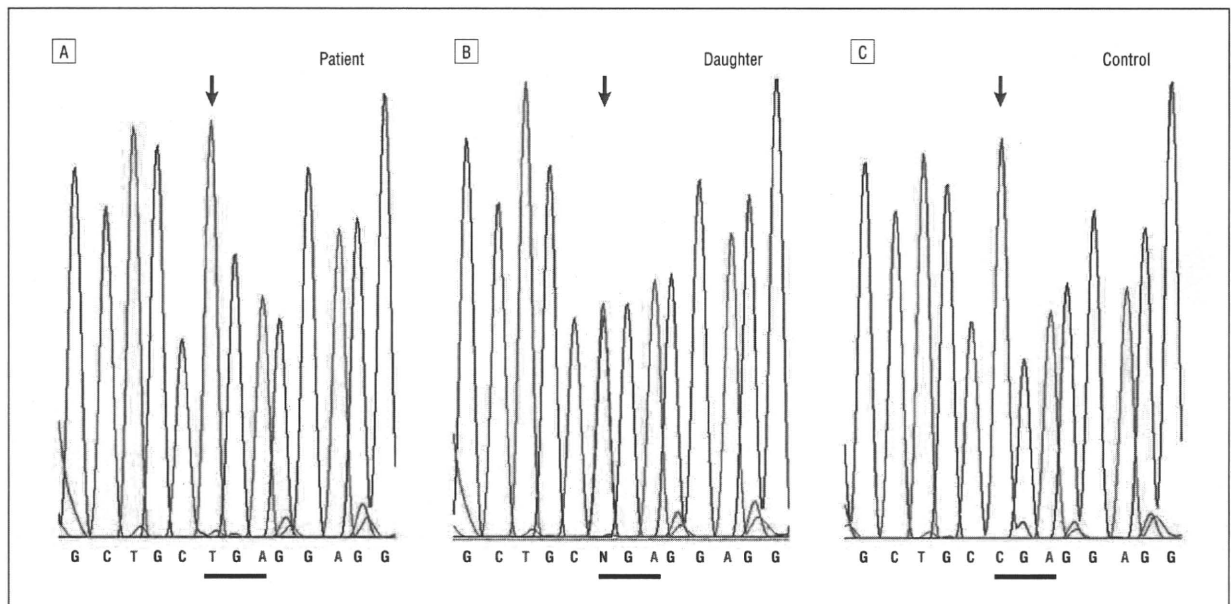
Figure 2. Sequence analysis of the *TAP2* gene. Detection of the mutation from genomic DNA was performed by polymerase chain reaction amplification of *TAP2* exon 3 for the patient (A) (mutant homozygous), a daughter (B) (heterozygous), and a healthy control (C) (native sequence).

previously ulcerated lesions of the right leg (Figure 1D and E), and the limb was amputated. The neoplasia recurred and metastasized, and the patient died.

Blood samples were obtained from the proband and relatives, and lymphocyte subpopulations were analyzed by flow cytometry. The numbers of NK cells, γδ T lymphocytes, and CD8$^+$ αβ T cells as well as the CD4/CD8 ratios were found to be normal and comparable to those found in controls and her relatives. The HLA I expression in the patient's lymphocytes was severely reduced (30 times lower than in healthy controls). The HLA serologic typing in the patient was unsuccessful. We extracted RNA from peripheral blood mononuclear cells; all coding exons of *TAP1* and *TAP2* genes (OMIM 170260 and 170261, respectively) were amplified by reverse transcriptase–PCR, and further sequencing analysis was performed. A previously unreported *TAP2* missense mutation was detected. The patient was homozygous for a C→T transition at nucleotide 628 (*TAP2* exon 3) (**Figure 2**), leading to a premature stop at codon 210 between the fifth and the sixth transmembrane domains of *TAP2*. Her mother and daughters were heterozygous for the mutated allele. In addition, high-resolution molecular HLA typing demonstrated that the patient was homozygous for the haplotype HLA-A*0301, Cw*1701, B*5001, DRB1*0301, DQA*0501/DQB1*0201, and DPB1*0401.

Comment. We report herein an SCC originating in a chronic ulcer of a patient with type I BLS and a novel *TAP2* gene mutation. Abnormal expression of HLA class I has been reported in many human neoplasias,[5] including skin cancer. Our findings suggest that TAP-impaired HLA class I expression could influence the course of SCC originating in chronic ulcers and could

be related to escape from cytotoxic T-lymphocyte surveillance during disease progression.

Agustín España, MD
Cecilia González-Santesteban, PhD
Laura Martínez-Martínez, PhD
Ana Bauzá, MD
Oscar de la Calle-Martín, PhD

Correspondence: Dr España, Department of Dermatology, University Clinic of Navarra, School of Medicine, University of Navarra, PO Box 4209, Pamplona, Navarra, Spain (aespana@unav.es).
**Financial Disclosure:** None reported.

1. de la Salle H, Hanau D, Fricker D, et al. Homozygous human TAP peptide transporter mutation in HLA class I deficiency. *Science.* 1994;265(5169):237-241.
2. Moins-Teisserenc HT, Gadola SD, Cella M, et al. Association of a syndrome resembling Wegener's granulomatosis with low surface expression of HLA class I-molecules. *Lancet.* 1999;354(9190):1598-1603.
3. Peaper DR, Cresswell P. Regulation of MHC class I assembly and peptide binding. *Annu Rev Cell Dev Biol.* 2008;24:343-368.
4. Zimmer J, Andres E, Donato L, Hanau D, Hentges F, de la Salle H. Clinical and immunological aspects of HLA class I deficiency. *QJM.* 2005;98(10):719-727.
5. Garrido F, Ruiz-Cabello F, Cabrera T, et al. Implications for immunosurveillance of altered HLA class I phenotypes in human tumours. *Immunol Today.* 1997;18(2):89-95.

Hereditary Benign Telangiectasia: Two Families With Punctate Telangiectasias Surrounded by Anemic Halos

Hereditary benign telangiectasia (HBT), one of the primary telangiectatic disorders, is characterized by various patterns of widespread cutaneous telangiectasias.[1,2] It is distinguished from hereditary hemorrhagic telangiectasia by the absence of recurrent bleeding and systemic involvement. Herein we describe

−202−
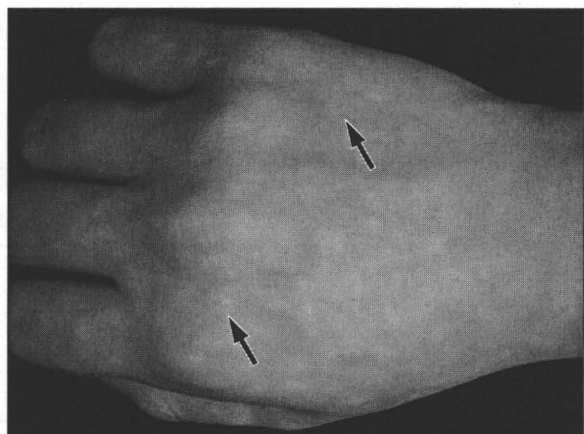
Figure 1. Skin lesions seen on the proband of family 1 with hereditary benign telangiectasia. Multiple punctate telangiectasias surrounded by anemic halos (arrows) are visible on the dorsal surface of the right hand.
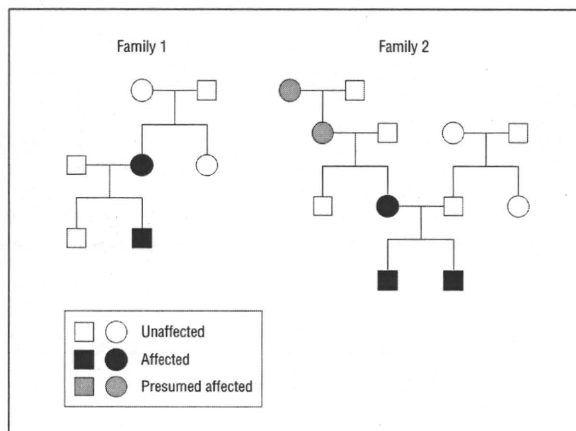

Figure 2. Pedigrees of the 2 families with hereditary benign telangiectasia showing punctate telangiectasias surrounded by anemic halos. Circles indicate female family members; squares, male family members.

2 families with HBT that show unique fine telangiectasias surrounded by anemic halos.

Report of Cases. *Case 1.* A 16-year-old boy was seen for asymptomatic telangiectasias with halos that had appeared several months earlier with no preceding episodes. Physical examination revealed multiple fine telangiectasias surrounded by pale macules as large as 5 mm on the dorsal surfaces of the hands (**Figure 1**), the radial aspects of the forearms and thighs, and on the trunk. The pale macules disappeared during application of mechanical pressure, which indicated that they were anemic halos. He also had numerous fine telangiectasias on the lips and irregularly shaped telangiectatic macules on the chest, right arm, and right thigh. His mother had similar fine telangiectasias surrounded by anemic halos on the right forearm (**Figure 2**). Laboratory data of the proband showed no abnormalities in blood cell count, liver function, renal function, or blood coagulation time. Skin specimens obtained from a telangiectasia with an anemic halo on the dorsal surface of the proband's hand demonstrated no specific changes. All of the telangiectatic lesions persisted for more than 5 years.

Case 2. A 14-year-old boy was referred for evaluation of asymptomatic fine telangiectasias surrounded by halos that had been noticed several weeks earlier without any preceding episodes. Multiple punctate telangiectasias surrounded by anemic halos were seen on the dorsal surfaces of the hands and on the radial aspects of the forearms. He had some irregularly shaped telangiectatic macules on the face, trunk, and extremities.

His mother had macular telangiectasias on her back and face, and his 11-year-old brother had similar lesions on his left hand and upper extremities (Figure 2). None of the family members had remarkable medical histories or hemorrhagic episodes. His maternal grandmother and great-grandmother seemed to have some reddish macular lesions, but the details were unclear (Figure 2).

No specific abnormalities were detected in laboratory examinations of the proband. Histologic and ultrastructural examinations of the biopsy specimens from the proband demonstrated no specific changes. To date, the cutaneous lesions of the proband remain unchanged for over 5 years.

Comment. Initially described in 1971,[2] HBT is probably an autosomal dominant disorder.[1] Various patterns of telangiectatic lesions, including plaquelike, radiating, arborizing, reticulated, mottled, spiderlike, and punctate, have been described in HBT.[1,2] Punctate telangiectasias surrounded by anemic halos have rarely been reported.[3] The mechanism whereby the anemic halo develops remains unclear. In eruptive pseudoangiomatosis, a rare skin disorder characterized by acute angiomalike papules or macules, the surrounding halo might be due to vasoconstriction around the vasodilatation of the papular angiomatous lesions.[4] In nevus anemicus, the anemic macule is thought to be caused by increased local vascular reactivity to catecholamines.[5] The findings from the families described herein indicate that punctate telangiectasias surrounded by anemic halos should be recognized as unique and characteristic features of HBT.

Hideyuki Ujiie, MD
Kazuo Kodama, MD, PhD
Masashi Akiyama, MD, PhD
Hiroshi Shimizu, MD, PhD

Correspondence: Dr Ujiie, Department of Dermatology, Hokkaido University Graduate School of Medicine, N15 W7, Kita-ku, Sapporo 060-8638, Japan (h-ujiie @med.hokudai.ac.jp).

1. Brancati F, Valente EM, Tadini G, et al. Autosomal dominant hereditary benign telangiectasia maps to the CMC1 locus for capillary malformation on chromosome 5q14. *J Med Genet.* 2003;40(11):849-853.
2. Ryan TJ, Wells RS. Hereditary benign telangiectasia. *Trans St Johns Hosp Dermatol Soc.* 1971;57(1):148-156.
3. Puppin D Jr, Rybojad M, Morel P. Hereditary benign telangiectasia: two case reports. *J Dermatol.* 1992;19(6):384-386.
4. Neri I, Patrizi A, Guerrini V, Ricci G, Cevenini R. Eruptive pseudoangiomatosis. *Br J Dermatol.* 2000;143(2):435-438.
5. Greaves MW, Birkett D, Johnson C. Nevus anemicus: a unique catecholamine-dependent nevus. *Arch Dermatol.* 1970;102(2):172-176.

−203−
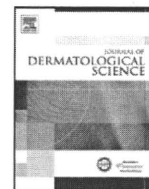
Epidermal triglyceride levels are correlated with severity of ichthyosis in Dorfman–Chanarin syndrome

Mayumi Ujihara [a], Kimiko Nakajima [a], Mayuko Yamamoto [a], Mika Teraishi [a], Yoshikazu Uchida [b], Masashi Akiyama [c], Hiroshi Shimizu [c], Shigetoshi Sano [a,*]

[a] Department of Dermatology, Kochi Medical School, Kochi University, Oko-cho, Nankoku, Japan
[b] Department of Dermatology, School of Medicine, University of California San Francisco, CA, USA
[c] Department of Dermatology, Hokkaido University Graduate School of Medicine, Sapporo, Japan

ABSTRACT

Background: Dorfman–Chanarin syndrome (DCS), also referred to as neutral lipid storage disease with ichthyosis, is a rare autosomal recessive form of nonbullous congenital ichthyosiform erythroderma, characterized by the presence of intracellular lipid droplets in multiorgans. DCS patients often have mutations in CGI-58, which is an activator of adipose triglyceride lipase (ATGL), leading to accumulation of triglycerides (TG).
Objective: To study whether a patient with DCS demonstrates TG accumulation in the epidermis and to analyze whether TG levels are correlated with skin disease activity.
Methods: Skin specimen from a 62-year-old man with DCS was stained with oil red O, and analyzed on electromicrographs. Sequencing analysis of CGI-58 was performed using the patient's blood cells. The scales from the lesion were subject to lipid analysis by high-performance thin-layer chromatography (HPTLC).
Results: The patient demonstrated ichthyoform erythroderma with a distinct seasonal fluctuation: his skin lesions were aggravated in summer but resolved during winter. Epidermis of the lesion showed intracellular lipid droplets. Sequencing analysis revealed a novel missense mutation in the exon 3 of CGI-58 gene. Lipid analysis of the scales from his lesions, compared with those from normal human control, revealed increased levels of triglycerides (TG) but, in turn, decreased levels of free fatty acids, suggesting dysfunction of adipose TG lipase. Notably, the TG levels in the scales from the patient were positively correlated with the severity of ichthyosis.
Conclusion: These results suggest that TG accumulation by epidermal keratinocytes directly contributes to ichthyosiform phenotype of DCS.

1. Introduction

Dorfman–Chanarin syndrome (DCS, MIM275630), also referred to as neutral lipid storage disease with ichthyosis (NLSDI), is a rare autosomal recessive disorder, in which an excess of triacylglycerols (TG) accumulates in various cells [1–3]. DCS is characterized by nonbullous congenital ichthyosiform erythroderma associated with the presence of cytoplasmic neutral lipid droplets in keratinocytes, as well as a variety of cells in the body including peripheral leukocytes (Jordans' anomaly) [4] and liver cells [5]. Therefore, extracutaneous manifestations of DCS include hepatomegaly (fatty liver), myopathy, cataract, sensoryneural deafness and other neurological symptoms. While cutaneous manifestation of DCS represented nonbullous congenital ichthyosiform erythroderma of mild to moderate severity, the clinical heterogeneity is present. For example, they included nonspecific ichthyosiform dermatosis with alopecia [5], sparing of the face [6], or even no erythematous change [7]. In addition, a case with DCS exhibited ichthyotic erythematous plaques, which frequently migrated as a clinical feature resembling erythrokeratoderma variabilis [8].

Mutations in CGI-58 gene, which is also called ABHD5 and encodes a member of α/β-hydrolase family of proteins, have been identified as a cause of DCS [9]. CGI-58 is an activator of adipose triglyceride lipase (ATGL) contributing to TG lipolysis [10,11], which depends on its association with perilipin [12]. CGI-58 mutations, therefore, abrogated lipolysis and induced a systemic accumulation of lipids droplets. CGI-58 gene is located on 3p21, encoding seven exons, and expressed in many tissues including

* Corresponding author. Tel.: +81 88880 2363; fax: +81 88880 2364.
E-mail address: sano.derma@kochi-u.ac.jp (S. Sano).

skin [9,13]. In patients with DCS, *CGI-58* mutations were associated with defective formation of lamellar granules [14]. Lipid micro-inclusions in lamellar granules formed a non-lamellar phase within the stratum corneum interstices, contributing to permeability barrier dysfunction characterized by ichthyosis in DCS [15]. To date, 16 mutations of *CGI-58* gene have been reported [16], and each of mutations affected the structure of CGI-58, leading to dysfunction of the downstream lipase ATGL. The mutations found in DCS include missense mutations, nonsense mutations, splice site mutations, a deletion or insertion in exons causing a frameshift and premature termination of translation [9,14]. For instance, forced expression of mutant *CGI-58* gene into an adipocyte cell line resulted in its inability to interact with perilipin, leading to mistargeting of CGI-58 to the lipid droplets [12]. Further, expression of functional CGI-58 in DCS fibroblasts restores lipolysis and reversed the abnormal TG accumulation [10].

Mutations in the gene encoding ATGL (*PNPLA2*) have been identified as the cause of neutral lipid storage disease with myopathy (NLSDM) [17]. NLSDM patients and ATGL-deficient mice exhibited DCS-like features associated with TG accumulation in multiple tissues including adipose tissue, muscle, heart and other organs, however, devoid of ichthyosis [18,17].

Therefore, the mutations in *CGI-58* gene result in development of ichthyosis in addition to abnormalities shared with NLSDM. This notion indicated that CGI-58 possessed an additional function required for lipid metabolism in the epidermis [17]. Previous studies demonstrated that the ultrastructure of DCS included abnormal lipid micro-inclusions within lamellar bodies and resulting lamellar/non-lamellar phase separation or clefts in the intercellular spaces of cornified layer [3,14,15]. Very recent study revealed that CGI-58 expression was increased during differentiation and localized in lamellar granules of keratinocytes and likely to be involved in barrier formation [13]. Given that TG is the content of lipid deposition in DCS, unsolved question is that the ultrastructural aberrancy in the epidermis is similar to other inherited, lipid storage diseases associated with ichthyosis, such as Refsum disease, Sjögren–Larsson syndrome [15]. Thus, no direct evidence has been shown regarding the link of TG deposition in the epidermis and ichthyosiform phenotype found in DCS.

In the present study, we demonstrate a DCS patient with a novel mutation of *CGI-58* gene in one allele, showing an abrupt, seasonal variation of ichthyosiform lesions. Biochemical study of his scales revealed the increased levels of TG, which was positively correlated with severity of ichthyosis.

2. Materials and methods

2.1. Patient

This study was approved by the Institute Ethical Review Board of the Kochi Medical School, Kochi University, and performed according to the Declaration of Helsinki Principles. Skin samples and scales were provided from a patient with DCS (see Section 3 for further details) and healthy donors with sunburn as controls.

2.2. Electron microscopic examination

The skin biopsy specimens were fixed with 2% glutaraldehyde in 0.1 M sodium cacodylate (pH 7.3) for 2 h at room temperature. The skin samples were post-fixed for 1 h at room temperature with 2% osmium tetroxide in 0.1 M cacodylate buffer. The samples were then dehydrated in a graded series of ethanol. Following dehydration, the samples were transferred to propylene oxide and embedded in Epon 812 (TAAB Laboratories Equipment, Berkshire, England). They were observed with a Hitachi H-7100 electron microscope (Hitachi High-Technologies, Tokyo, Japan).

2.3. Determination of TEWL and water holding capability

To assess basal permeability barrier function, we used a Tewameter (TEWAMETER TM300, Courage and Khazaka, Cologne, Germany) over six separate sites. Water holding capability was determined using a corneometer (CORNEOMETER CM825, Courage and Khazaka) over six separate sites.

2.4. Mutation analysis

The method for mutation detection of *CGI-58* gene was performed as previously reported [9]. Briefly, genomic DNA isolated from peripheral blood was subject to PCR amplification, followed by direct automated sequencing. Oligonucleotide primers used for amplification of all exons 1–7 of *CGI-58* gene and detailed PCR conditions were described elsewhere [14,9].

2.5. Lipid analysis of scales

Total lipids were extracted from scales as described previously [19]. Scales from sunburn in a healthy individual were used as control for this assay, since we confirmed that its lipid content did not significantly differ from that previously reported from non-sunburn scales in normal donors. The individual lipid species were separated by high-performance thin-layer chromatography (HPTLC), followed by quantification by scanning densitometry as described previously with the following solvent systems: (1) benzene–n-hexane (1:1) to 8.5 cm; and n-hexane-diethyl ether–acetic acid (70:30:1, v/v/v) to 5 cm. Lipids were visualized after treatment with cupric acetate–phosphoric acid, and heating to 160 °C for 15 min. The quantity of each lipid was determined by spectrodensitometry, as previously described [19].

3. Results

3.1. Case presentation

A 62-year-old Japanese man visited our hospital in October 2006 complaining of slightly pruritic, dry skin with scaling. From early childhood the patient had been suffering from scaly skin lesions over the entire body, which were characterized by a seasonal variation with a marked aggravation in summer. He was the first and an only child from non-consanguineous parents. There was no family history of congenital ichthyosis or abnormal lipid diseases. The patient was mildly obese with a BMI 26.5 (height: 157 cm, weight: 65 kg). His skin was dry and mildly erythrodermic with fine scales, surrounding normal-looking skin with irregular patterns on the trunk, lateral side of upper arms, the right scapular region, bilateral breasts, and buttocks (Fig. 1a and b). The skin of the dorsa of the hands was shiny with prominent creases and lamellar scaling was in lower legs (Fig. 1c). There were spiny keratoses on his palms, but the nails, teeth and hair appeared normal.

Transepidermal water loss (TEWL) and skin hydration were assessed in the involved skin and normal-looking, uninvolved skin of the upper arm. TEWL of the ichthyosiform lesion ($18.0 \text{ g h}^{-1} \text{ m}^{-2}$) was within the normal range (0–10, very good; 10–15, good; 15–20, fair; 25–30, poor; more than 30, very poor) but slightly higher than uninvolved skin ($14.5 \text{ g h}^{-1} \text{ m}^{-2}$). On the other hand, the water retention capability was markedly impaired in the lesion (6.7, normal >60) compared with the uninvolved skin (63.8). These results indicated that the ichthyosiform lesions of this patient showed an intact permeability barrier but a markedly decreased hydration, which was contrast to a previous study showing abnormal barrier function [15].
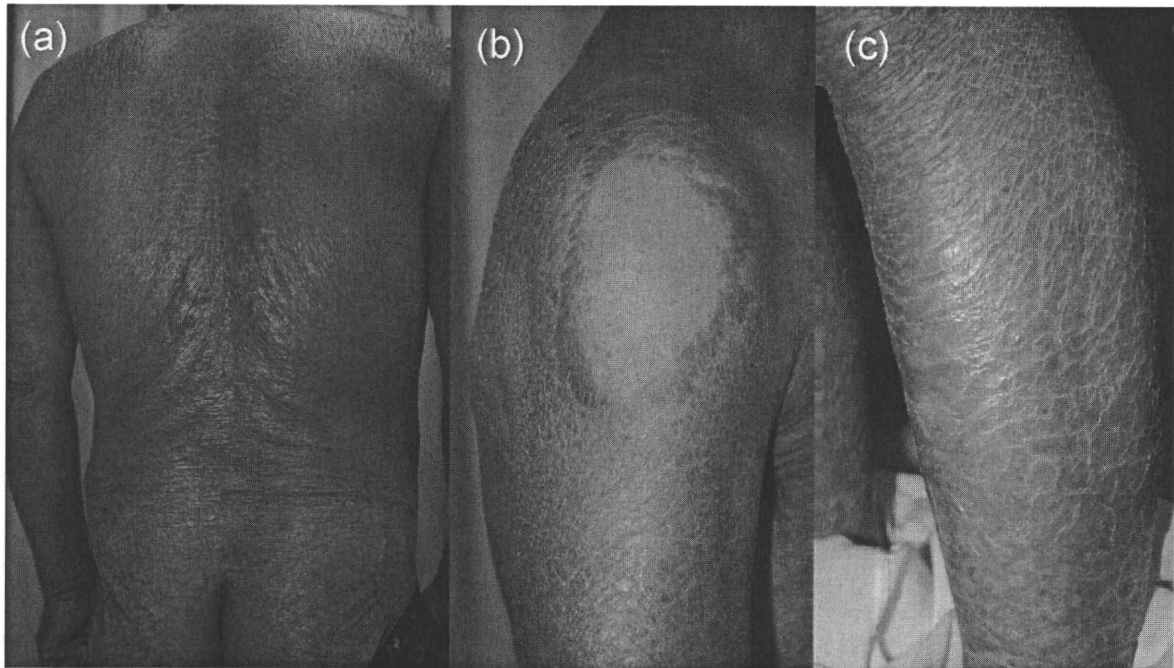
Fig. 1. Clinical appearance. (a) Scaly ichthyosiform erythroderma. (b) Sharply demarcated site of uninvolved skin on the lateral aspect of the upper arm. (c) Large, membranous scales on the legs.

Laboratory investigation revealed abnormalities of hepatic enzymes including aspartate aminotransferase 85 IU L^{-1} (normal range: 10–35), alanine aminotransferase 79 IU L^{-1} (5–40), γ-glutamyltransferase 497 IU L^{-1} (5–70), and alkaline phosphatase 366 IU L^{-1} (100–344). The computed tomography and ultrasonic examination demonstrated hepatic hypertrophy and fatty liver. Steroid sulfatase activity in the peripheral blood sample was normal. Although white blood cell count was normal, there were distinct intracytoplasmic vacuoles in polynuclear leukocytes (Fig. 2c) and monocytes (Fig. 2d), which were presumed to be

Jordan's anomaly [4]. No evidence of muscle weakness or neurological abnormality was obtained.

3.2. Histologic features and lipid droplets in the epidermis

Skin biopsy specimen from the right thigh revealed hyperkeratosis and mild acanthosis but the granular layer was normal (Fig. 2a). There were mild mononuclear cell infiltrates around blood vessels in the dermis. Groups and strands of fat cells were found embedded among the proliferating collagen bundles of the
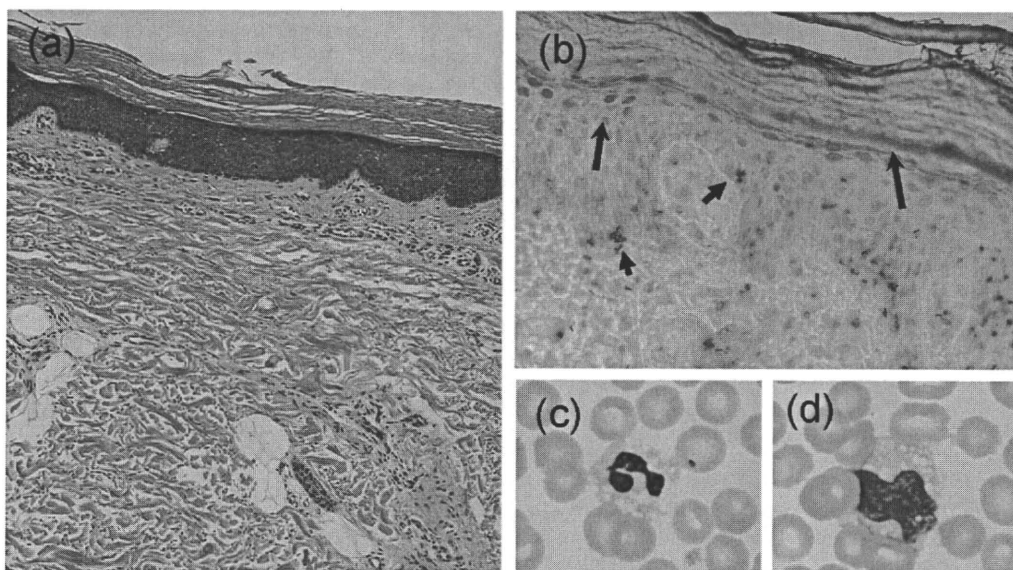
Fig. 2. Histologic appearance and lipid deposition in epidermis and white blood cells. (a) H&E staining of formalin-fixed, paraffin-embedded lesional skin section from the patient's left thigh. Hyperkeratosis, acanthosis and mild perivascular infiltrates are noted (40×). (b) Oil red O staining of frozen section (200×). The cornified and granular layers are strongly stained with oil red O (arrows), which also stained cells of basal layer in punctate (arrowheads). Intracytoplasmic vacuoles within peripheral blood neutrophils (c, 1000×) and monocytes (d, 1000×) represent Jordan's anomaly.
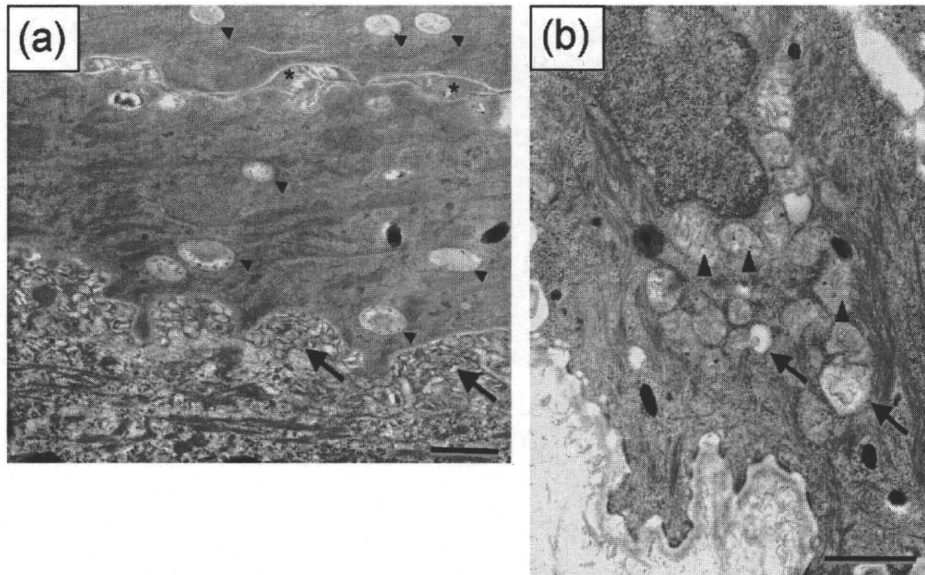
Fig. 3. Electron micrographs after osmium tetroxide post-fixation and Epon embedding. (a) Electron-lucent vacuoles are present within corneocytes (arrowheads). There are amorphous materials in the intracellular spaces (asterisks). Abnormal lamellar granules are aggregated in the stratum granulosum/stratum corneum interface (arrows). Scale bar, 0.5 μm. (b) Giant mitochondria (arrowheads) and lucent vacuoles (arrows) are seen in the cytoplasm of basal cells. Scale bar, 1 μm.

dermis (Fig. 2a). Staining with oil red O demonstrated lipid droplets within keratinocytes in the stratum granulosum, the stratum corneum (Fig. 2b, arrows) and the basal layer (Fig. 2b, arrowheads). Taken together, we diagnosed him as DCS.

3.3. Ultrastructural findings

Electron microscopic examination of the lesional skin of the patient revealed a number of electron-lucent vacuoles, presumably lipid droplets, within the cytoplasm of corneocytes and deposits of amorphous materials in the intercellular spaces (Fig. 3a). Accumulation of abnormal lamellar granules lacking the normal lamellar content was also seen in the stratum granulosum/stratum corneum interface (arrows in Fig. 3a). These features were consistent with previous studies with DCS [14,15]. Furthermore, giant mitochondria and lucent vacuoles were found within the basal keratinocytes (Fig. 3b), suggesting an abnormal lipid metabolism of keratinocytes as previously described [20].

Fig. 4. Sequencing analysis of *CGI-58* gene. A novel heterozygous 215T>C transition in the exon 3, that substitutes isoleucine for threonine at position 72 (I72T).

3.4. Mutation in CGI-58 gene

Mutation analysis of *CGI-58* gene of the patient's blood revealed a heterozygous point mutation (215T>C) in the exon 3 (Fig. 4). This novel mutation substituted isoleucine for threonine at position 72 (Ile72Thr), indicating a missense mutation. However, further analysis of another allele failed to detect any other pathogenic mutation within the all seven exons and exon–intron borders of this gene (data not shown).

3.5. Seasonal variation of disease activity

Notably, his skin lesions were aggravated in summer. As shown in Fig. 5, the ichthyosiform lesions recurred with some irritant sensation in the beginning of April every year, and developed keratotic erythrodermia before summer. The ichthyosiform lesions spread over entire body, but several areas were spared, for example, around nipples. This manifestation was very similar to a previous report, in which a patient with DCS showed erythematous migratory patches resembling erythrokeratoderma variabilis [8]. With lowering the air temperature in autumn, the ichthyosiform plaques were remitted, and mostly, if any, disappeared by mid-winter. Interestingly, his skin lesions showed some resolution when he stayed away from hot temperature even in the mid-summer, but were immediately aggregated when stayed outside. This suggested that the development of the ichthyosiform change was dependent on environmental temperature. Such feature was also similar to the aforementioned DCS patient [8].

3.6. Lipid analysis of scales

Scales were collected from the involved sites of the patient at aggravation and remission stages. Scales from a non-ichthyotic individual with sunburn dermatitis were used as a control. Although there was no difference in the quantity of cholesterol between the patient and control, triglycerides (TG) were increased by two- and threefold over control in the scales at remission and aggravation stage, respectively (Fig. 6). Thus, TG levels in scales were correlated with the severity of ichthyotic condition. In
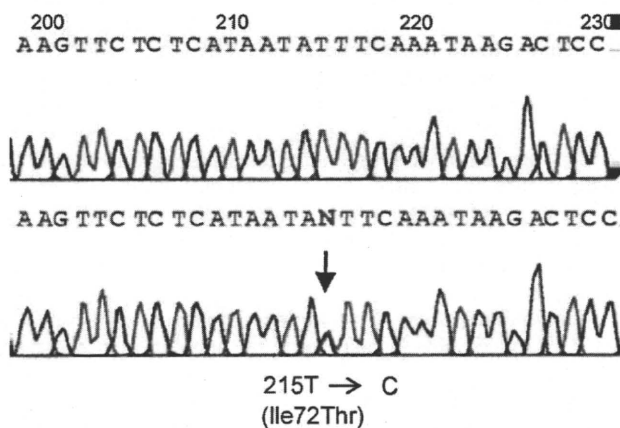
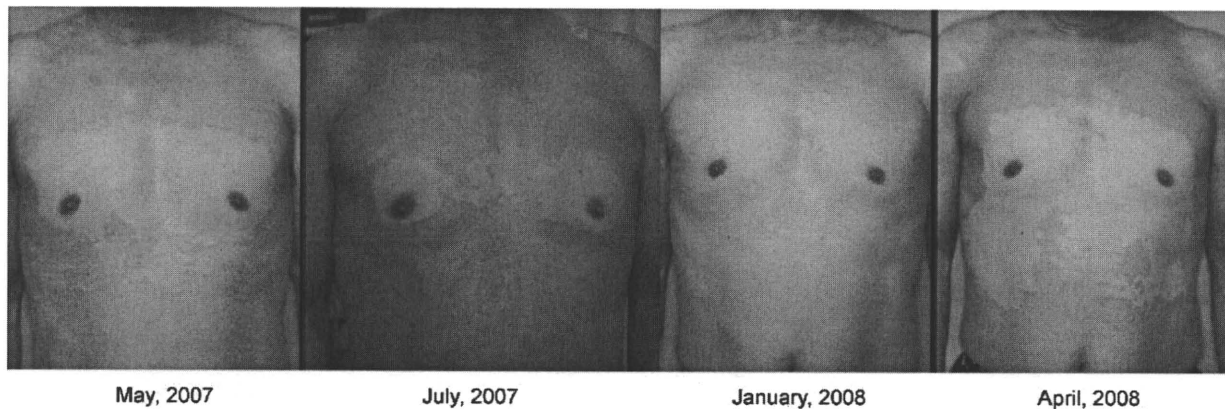May, 2007   July, 2007   January, 2008   April, 2008

Fig. 5. Distinct seasonal variation of ichthyosis. Ichthyosiform lesions were aggravated from spring and formed erythroderma throughout hot season, but ameliorated in winter.
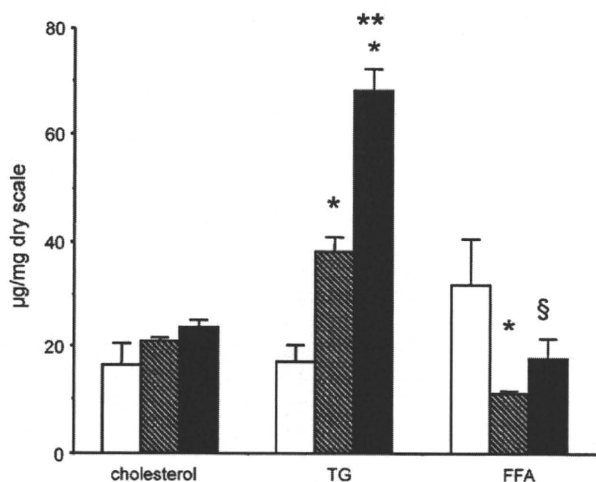

Fig. 6. Lipid analysis of scales taken from sunburn lesion as controls (white bar), patient's lesions at aggravation and remission stages (black, shaded bars, respectively), showing positive correlation of increased TG levels with disease severity. FFA levels are invariably decreased in patient's scales. Mean ± s.d. μg/mg dry scale. $*p < 0.01$ vs. control. $**p < 0.01$ vs. remission stage. $§p < 0.02$ vs. control.

contrast, free fatty acids were invariably decreased in the patient's scales compared with control. These results were relevant, since DCS is characterized by dysfunction of CGI-58, an activator of ATGL, which hydrolyzes TG to release FFA.

4. Discussion

Dorfman–Chanarin syndrome (DCS) is defined as a neutral lipid storage disorder with ichthyosis (NLSDI), which is attributed to mutations in CGI-58. Since CGI-58 is an activator of adipose triglyceride lipase (ATGL), patients with DCS demonstrated systemic storage of triglycerides as found in patients with mutations in ATGL, which were designated a neutral lipid storage disorder with myopathy (NLSDM). However, NLSDM patients and ATGL-deficient mice did not develop ichthyosis [17,18]. It was, therefore, hypothesized that CGI-58 could have an additional metabolic function required for normal skin physiology [17]. This hypothesis was supported by the fact that the lipid accumulation in the epidermis was higher in DCS than in NLSDM [17].

Sequencing analysis of the CGI-58 gene using the patient's blood cells revealed a novel missense mutation in nucleotide position 215 (T>C) within the exon 3. As far as we examined, however, no mutation of this gene was found in another allele. Moreover, RT-PCR using primer sets specific for some exons including the exon 3 demonstrated no mRNA alteration in quantity and size compared to healthy controls (data not shown). Therefore, it was unlikely that truncation or instability of this gene occurred in our patient. His family history suggested that the inheritance was recessive, although there was no DCS patient among his relatives. It remained unsolved whether he had another undefined mutation of the CGI-58 in another allele (compound heterozygous) or whether he harboured any posttransriptional alteration in this gene. Recent findings of the CGI-58 gene expanded the clinical and mutational spectrum and underlie the genetic heterogeneity of this disease [21]. Alternatively, unknown mutations of other gene including the ATGL gene, might play a role [10], since mutations of CGI-58 were not invariably found in clinically typical patients with DCS [15,17].

In the present study, a lipid analysis of scales from the DCS patient revealed elevated TG levels in the epidermis, which was correlated with the clinical severity of ichthyosis. A decrease in FFA levels in the epidermis could be also attributed to a dysfunction of ATGL in this patient. Since cholesterol, ceramides, and FFA comprise intercellular lipids of the stratum corneum, a decrease in FFA levels could affect the integrity of the cornified layer [22,23]. These abnormalities might contribute to development of ichthyosis in this patient. It is, however, unclear why permeability barrier remained intact in our patient, while the water holding capacity was markedly decreased in the involved lesions. Akiyama and coworkers recently demonstrated that CGI-58 knockdown reduced expression of keratinocyte differentiation markers including filaggrin [13], which plays an important role in retaining stratum corneum water.

New pieces of puzzle come from the finding of seasonal fluctuation of ichthyosis severity in this patient and a previous case [8], presumably depending on the environmental temperature. In both cases, summer was an aggravating season. Elevation of temperature might affect the ATGL activity, if any left, or other lipolysis pathways, for example, the hormone sensitive lipase-dependent pathway [18]. Therefore, it should be clarified how the mutated CGI-58 in our patient impaired the ATGL, and whether ATGL, if any, or other compensatory lipase activity were temperature-sensitive. Haemmerle et al. have demonstrated that ATGL$^{-/-}$ mice showed defective cold adaptation because they could not produce FFAs to fuel thermogenesis [18]. We assume that ATGL activity could be decreased upon elevated environmental temperature because relatively reduced requirement of FFAs to be provided. In a patient like our case, impaired CGI-58 activity further might attenuate the ATGL activity at high temperature. To

verify this, lipase activity assay from the patient's cells will be required to see whether heat stimulation worsens it, which would be reversed by introduction of wild-type *CGI-58* gene.

Acknowledgments

References

[1] Dorfman ML, Hershko C, Eisenberg S, Sagher F. Ichthyosiform dermatosis with systemic lipidosis. Arch Dermatol 1974;110:261–6.

[2] Chanarin I, Patel A, Slavin G, Wills EJ, Andrews TM, Stewart G. Neutral-lipid storage disease: a new disorder of lipid metabolism. Br Med J 1975;1:553–5.

[3] Elias PM, Williams ML. Neutral lipid storage disease with ichthyosis. Defective lamellar body contents and intracellular dispersion. Arch Dermatol 1985;121:1000–8.

[4] Rozenszajn L, Klajman A, Yaffe D, Efrati P. Jordans' anomaly in white blood cells. Report of case. Blood 1966;28:258–65.

[5] Pena-Penabad C, Almagro M, Martinez W, Garcia-Silva J, Del Pozo J, Yebra MT, et al. Dorfman–Chanarin syndrome (neutral lipid storage disease): new clinical features. Br J Dermatol 2001;144:430–2.

[6] Srebrnik A, Brenner S, Ilie B, Messer G. Dorfman–Chanarin syndrome: morphologic studies and presentation of new cases. Am J Dermatopathol 1998;20:79–85.

[7] Srebrnik A, Tur E, Perluk C, Elman M, Messer G, Ilie B, et al. Dorfman–Chanarin syndrome. A case report and a review. J Am Acad Dermatol 1987;17:801–8.

[8] Pujol RM, Gilaberte M, Toll A, Florensa L, Lloreta J, Gonzalez-Ensenat MA, et al. Erythrokeratoderma variabilis-like ichthyosis in Chanarin–Dorfman syndrome. Br J Dermatol 2005;153:838–41.

[9] Lefevre C, Jobard F, Caux F, Bouadjar B, Karaduman A, Heilig R, et al. Mutations in CGI-58, the gene encoding a new protein of the esterase/lipase/thioesterase subfamily, in Chanarin–Dorfman syndrome. Am J Hum Genet 2001;69:1002–12.

[10] Lass A, Zimmermann R, Haemmerle G, Riederer M, Schoiswohl G, Schweiger M, et al. Adipose triglyceride lipase-mediated lipolysis of cellular fat stores is activated by CGI-58 and defective in Chanarin–Dorfman syndrome. Cell Metab 2006;3:309–19.

[11] Yen CL, Farese Jr RV. Fat breakdown: a function for CGI-58 (ABHD5) provides a new piece of the puzzle. Cell Metab 2006;3:305–7.

[12] Yamaguchi T, Omatsu N, Matsushita S, Osumi T. CGI-58 interacts with perilipin and is localized to lipid droplets. Possible involvement of CGI-58 mislocalization in Chanarin–Dorfman syndrome. J Biol Chem 2004;279:30490–7.

[13] Akiyama M, Sakai K, Takayama C, Yanagi T, Yamanaka Y, McMillan JR, et al. CGI-58 is an alpha/beta-hydrolase within lipid transporting lamellar granules of differentiated keratinocytes. Am J Pathol 2008;173:1349–60.

[14] Akiyama M, Sawamura D, Nomura Y, Sugawara M, Shimizu H. Truncation of CGI-58 protein causes malformation of lamellar granules resulting in ichthyosis in Dorfman–Chanarin syndrome. J Invest Dermatol 2003;121:1029–34.

[15] Demerjian M, Crumrine DA, Milstone LM, Williams ML, Elia PM. Barrier dysfunction and pathogenesis of neutral lipid storage disease with ichthyosis (Chanarin–Dorfman syndrome). J Invest Dermatol 2006;126:2032–8.

[16] Ben Selma Z, Yilmaz S, Schischmanoff PO, Blom A, Ozogul C, Laroche L, et al. A novel S115G mutation of CGI-58 in a Turkish patient with Dorfman–Chanarin syndrome. J Invest Dermatol 2007;127:2273–6.

[17] Fischer J, Lefevre C, Morava E, Mussini JM, Laforet P, Negre-Salvayre A, et al. The gene encoding adipose triglyceride lipase (PNPLA2) is mutated in neutral lipid storage disease with myopathy. Nat Genet 2007;39:28–30.

[18] Haemmerle G, Lass A, Zimmermann R, Gorkiewicz G, Meyer C, Rozman J, et al. Defective lipolysis and altered energy metabolism in mice lacking adipose triglyceride lipase. Science 2006;312:734–7.

[19] Uchida Y, Behne M, Quiec D, Elias PM, Holleran WM. Vitamin C stimulates sphingolipid production and markers of barrier formation in submerged human keratinocyte cultures. J Invest Dermatol 2001;117:1307–13.

[20] Hashimoto K, Khan S. Harlequin fetus with abnormal lamellar granules and giant mitochondria. J Cutan Pathol 1992;19:247–52.

[21] Bruno C, Bertini E, Di Rocco M, Cassandrini D, Ruffa G, De Toni T, et al. Clinical and genetic characterization of Chanarin–Dorfman syndrome. Biochem Biophys Res Commun 2008;369:1125–8.

[22] Grubauer G, Feingold KR, Elias PM. Relationship of epidermal lipogenesis to cutaneous barrier function. J Lipid Res 1987;28:746–52.

[23] Mao-Qiang M, Elias PM, Feingold KR. Fatty acids are required for epidermal permeability barrier function. J Clin Invest 1993;92:791–8.

Neutral Lipid Storage Leads to Acylceramide Deficiency, Likely Contributing to the Pathogenesis of Dorfman–Chanarin Syndrome

TO THE EDITOR

Dorfman–Chanarin syndrome (DCS) is an autosomal recessive, neutral lipid storage disorder with ichthyosis (NLSDI) due to loss-of-function mutations in CGI-58 (a/β-hydrolase domain-containing protein 5, ABHD5). CGI-58 encodes a 39 kDa protein, a widely expressed cofactor in mammalian tissues including epidermis that activates adipose triglyceride (TG) lipase (reviewed in Schweiger et al., 2009; Yamaguchi and Osumi, 2009), as well as other still unidentified TG lipases (Radner et al., 2009). CGI-58 expression increases during keratinocyte differentiation; and conversely, knockdown of this cofactor reduces keratinocyte differentiation (Akiyama et al., 2008). Epidermal permeability barrier defects due in part to lamellar/nonlamellar phase separation of secreted lipids, within extracellular domains of the stratum corneum (SC) have been proposed to account for the barrier abnormalities in NLSDI (Elias and Williams, 1985; Demerjian et al., 2006). Although defective extracellular lipid organization clearly is one contributor (Demerjian et al., 2006), we assessed whether diversion of free fatty acid (FA) into esterified lipids causes lipid abnormalities that further impact barrier formation.

We recently reported a DCS patient with a, to our knowledge, previously unreported CGI-58 missense mutation (Ujihara et al., 2010), exhibiting abnormal barrier-related structures resembling other NLSDI patients (Demerjian

et al., 2006). Both mild and severely affected ichthyotic SCs revealed increased TG and decreased FA levels in comparison with SC fraction from normal subjects (Ujihara et al., 2010). Pertinently, the extent of the increase in TG levels correlated with site-specific differences in the severity of the dermatosis (Ujihara et al., 2010). These observations suggest that divergence of FA to TG contributes to disease phenotype in NLSDI.

We previously showed that ω-O-acylceramides (or acylCer) that have only been identified in differentiated layers of epidermis in terrestrial mammals are essential constituents of the epidermal permeability barrier; that is, lack of acylCer formation results in neonatal death due to abnormal epidermal permeability barrier function (Vasireddy et al., 2007). AcylCer and the de-ω-O-esterified form (ω-hydroxy [ω-OH] ceramide [Cer]) are present either as free (unbound) or bound species (Uchida and Holleran, 2008). The latter form a continuous lipid monolayer, the corneocyte-bound lipid envelope (CLE); that is, a pool of ω-OH Cer, which is covalently bound to the external surface of the cornified envelope (Uchida and Holleran, 2008). Although free acylCer are critical for the formation of the lamellar membranes (Bouwstra et al., 1998), our previous studies suggest the CLE is also important for normal permeability barrier function (Behne et al., 2000). Prior studies suggest that FAs derived from TG are used in the

ω-O-esterification step to form acylCer (Wertz and Downing, 1990). Moreover, TG, linoleate, and acylCer, but not phosphoglycerolipid content, decline in acyl-CoA: diacylglycerol acyltransferase-2-deficient mice, which also show a permeability barrier abnormality (Stone et al., 2004). In addition, linoleate, which is the predominant FA that is used for ω-O-esterification, is enriched in TG in mouse skin (Stone et al., 2004). Thus, we hypothesized that a failure of TG hydrolysis, due to abnormal CGI-58 function, could attenuate permeability barrier formation in NLSDI by decreasing acylCer content of affected SC.

Therefore, we first investigated the lipid profiles in solvent extracts of SC from this DCS patient (Ujihara et al., 2010). Neither cholesterol (Ujihara et al., 2010) nor total (bulk) Cer (Figure 1a) content was altered. Yet, Cer comprises a family of at least 10 species in humans (Uchida and Holleran, 2008). Because not only bulk Cer amount but also each individual Cer species contributes to the formation of competent lamellar structures required for barrier function (Bouwstra et al., 1998), we subfractionated Cer into individual Cer species. Whereas the major Cer subfractions, NS (Cer 2), NP (Cer 3), and AS (Cer 5) were not significantly altered, acylCer were present at only trace levels in the patient sample (Figure 1b; because sample amounts were limited, other minor Cer species; that is, EOH (Cer 4), AP (Cer 6) (AP), AH (Cer 7) could not be quantitated) (abbreviations for Cer structures are according to Motta. et al. and Robson K. et al., details reviewed in Uchida and Holleran, 2008).
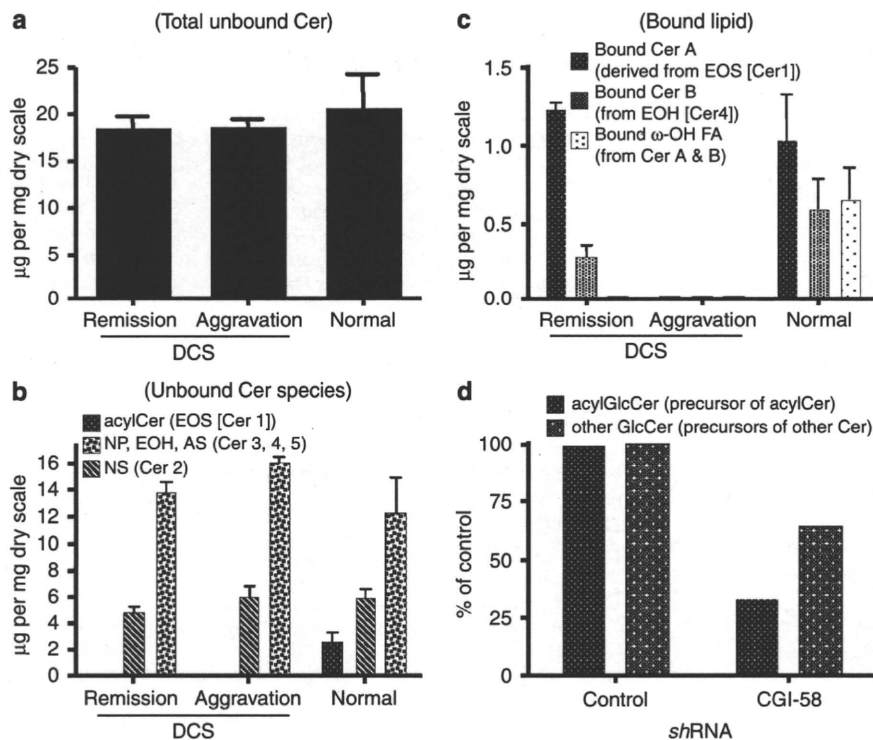
Figure 1. Lipid profile in the stratum corneum. Both unbound acylCer and bound ω-OH Cer deficiencies occur in a Dorfman–Chanarin syndrome (DCS) stratum corneum (SC) (**a–c**), whereas diminished CGI-58 expression decreases acylglucosylCer production (**d**). Normal SC from sunburn lesion as controls. CHK transfected with lentivirus-expressed shRNA (CGI-58 or control vector) were cultured in differentiation-inducing medium (Uchida *et al.*, 2001). Lipids were isolated from SC or cells and quantitated using thin-layer chromatography-scanning densitometry as described previously (Uchida *et al.*, 2001). *n* = 1 (DC) and *n* = 3 (normal). All studies were approved by the institutional ethics review boards (Kochi University and University of California, San Francisco) and were performed according to the Declaration of Helsinki Principles.
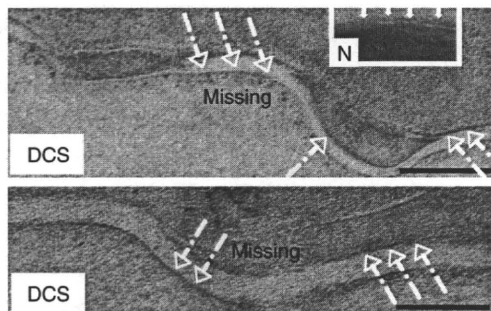
Figure 2. Electron micrographs display lack of continuous lipid monolayer, CLE, in the SC from two DCS patients (Demerjian *et al.*, 2006) vs. normal subject (inset, N). Skin samples were fixed in Karnovsky's fixative, and post-fixed with ruthenium tetroxide or osmium tetroxide, as previously described (Behne *et al.*, 2000). Ultrathin sections were examined, after further contrasted with lead citrate, with a Zeiss 10A (Carl Zeiss, Thornwood, NY) (Behne *et al.*, 2000). Arrows (with solid line, presence and with dotted line, absence) indicate CLE structures. Bars = 100 nm.

Not only bound ω-OH Cer, but also bound ω-OH FA (resulting from the subsequent hydrolysis of some bound ω-OH Cer by ceramidase) decline significantly in DCS (Figure 1c). As with TG accumulation (Ujihara *et al.*, 2010), the decrease in these bound lipids reflects disease severity. Accordingly,

this patient, as well as in two additional DCS patients (Demerjian *et al.*, 2006), lacked CLE on ultrastructural analysis of affected SC (Figure 2).

Finally, we investigated whether the decreased acylCer in DCS is due to a gain-of-function of mutation in *CGI-58*, rather than a deficiency of

TG-derived FA. A substantial decrease in acylglucosylCer (= acylCer precursor), but not in other glucosylCer species, was evident in lentivirus-expressed CGI-58 shRNA-treated cultured human keratinocytes (Figure 1d). Hence, by facilitating the lipolysis of TG, CGI-58 provides FA for ω-*O*-esterification leading to acylCer formation. The recent demonstration of a lethal, postnatal permeability barrier defect and deficiency of both acylCer and bound ω-OH Cer in *cgi-58*-null mice (Radner *et al.*, 2009) further supports this conclusion.

We conclude from these and previous studies that CGI-58 not only facilitates TG lipolysis but also provides FA for the ω-*O*-esterification of Cer leading to acylCer production, as well as bound ω-OH Cer generation leading to CLE formation (see Supplementary Figure S1 online). These studies highlight that the deficiency of an essential barrier constitute, acylCer, likely contributes to the permeability barrier

abnormality in DCS. Although the function of the CLE is still unclear, a role as a necessary scaffold for the lamellar bilayer organization is likely (Uchida and Holleran, 2008). Thus, CLE deficiency, coupled with disorganization of extracellular lamellar bilayers, likely merge to provoke the barrier abnormality in NLSDI (see Supplementary Figure S2 online). Finally, to overcome this metabolic disadvantage in forming the epidermal permeability barrier, epidermal proliferation likely increases, which in turn results in hyperkeratosis, phenotypic features common to virtually all of the ichthyoses (Demerjian et al., 2006; Akiyama et al., 2008), that is, 'A compromised permeability barrier 'drives' the hyperproliferative epidermis in NLSDI and other ichthyoses' (Elias et al., 2008).

CONFLICT OF INTEREST
The authors state no conflict of interest.

Yoshikazu Uchida[1,2], Yunhi Cho[1,2,3], Sam Moradian[1,2], Jungmin Kim[1,2,3], Kimiko Nakajima[4], Debra Crumrine[1,2], Kyungho Park[1,2], Mayumi Ujihara[4], Masashi Akiyama[5], Hiroshi Shimizu[5], Walter M. Holleran[1,2,6], Shigetoshi Sano[4] and Peter M. Elias[1,2]

[1]Department of Dermatology, School of Medicine, University of California, San Francisco, San Francisco, California, USA; [2]Department of Veterans Affairs Medical Center and Northern California Institute for Research and Education, San Francisco, California, USA; [3]Department of Medical Nutrition, Graduate School of East-West Medical Science, Kyung Hee University, Seoul, South Korea; [4]Department of Dermatology, Kochi Medical School, Kochi University, Nankoku, Japan; [5]Department of Dermatology, Hokkaido University Graduate School of Medicine, Sapporo, Japan and [6]Department of Pharmaceutical Chemistry, School of Pharmacy, University of California, San Francisco, San Francisco, California, USA
E-mail: uchiday@derm.ucsf.edu

REFERENCES
Akiyama M, Sakai K, Takayama C et al. (2008) CGI-58 is an alpha/beta-hydrolase within lipid transporting lamellar granules of differentiated keratinocytes. Am J Pathol 173:1349–60

Behne M, Uchida Y, Seki T et al. (2000) Omega-hydroxyceramides are required for corneocyte lipid envelope (CLE) formation and normal epidermal permeability barrier function. J Invest Dermatol 114:185–92

Bouwstra JA, Gooris GS, Dubbelaar FE et al. (1998) Role of ceramide 1 in the molecular organization of the stratum corneum lipids. J Lipid Res 39:186–96

Demerjian M, Crumrine DA, Milstone LM et al. (2006) Barrier dysfunction and pathogenesis of neutral lipid storage disease with ichthyosis (Chanarin–Dorfman syndrome). J Invest Dermatol 126:2032–8

Elias PM, Williams ML (1985) Neutral lipid storage disease with ichthyosis. Defective lamellar body contents and intracellular dispersion. Arch Dermatol 121:1000–8

Elias PM, Williams ML, Holleran WM et al. (2008) Pathogenesis of permeability barrier abnormalities in the ichthyoses: inherited disorders of lipid metabolism. J Lipid Res 49:697–714

Radner FP, Streith IE, Schoiswohl G et al. (2009) Growth retardation, impaired triacylglycerol catabolism, hepatic steatosis, and lethal skin barrier defect in mice lacking comparative gene identification-58 (CGI-58). J Biol Chem 285:7300–11

Schweiger M, Lass A, Zimmermann R et al. (2009) Neutral lipid storage disease: genetic disorders caused by mutations in adipose triglyceride lipase/PNPLA2 or CGI-58/ABHD5. Am J Physiol Endocrinol Metab 297:E289–96

Stone SJ, Myers HM, Watkins SM et al. (2004) Lipopenia and skin barrier abnormalities in DGAT2-deficient mice. J Biol Chem 279:11767–76

Uchida Y, Behne M, Quiec D et al. (2001) Vitamin C stimulates sphingolipid production and markers of barrier formation in submerged human keratinocyte cultures. J Invest Dermatol 117:1307–13

Uchida Y, Holleran WM (2008) Omega-O-acylceramide, a lipid essential for mammalian survival. J Dermatol Sci 51:77–87

Ujihara M, Nakajima K, Yamamoto M et al. (2010) Epidermal triglyceride levels are correlated with severity of ichthyosis in Dorfman–Chanarin syndrome. J Dermatol Sci 57:102–7

Vasireddy V, Uchida Y, Salem Jr N et al. (2007) Loss of functional ELOVL4 depletes very long-chain fatty acids (>=C28) and the unique {omega}-O-acylceramides in skin leading to neonatal death. Hum Mol Genet 16:471–82

Wertz PW, Downing DT (1990) Metabolism of linoleic acid in porcine epidermis. J Lipid Res 31:1839–44

Yamaguchi T, Osumi T (2009) Chanarin–Dorfman syndrome: deficiency in CGI-58, a lipid droplet-bound coactivator of lipase. Biochim Biophys Acta 1791:519–23

Detection of Human Papillomavirus DNA in Plucked Eyebrow Hair from HIV-Infected Patients

TO THE EDITOR
The risk of developing human papillomavirus (HPV)-related benign and malignant cutaneous lesions is markedly increased in immunosuppressed people such as organ-transplant recipients (Harwood et al., 2000) and HIV-infected patients (Grulich et al., 2007; Stier and Baranoski, 2008). Although HPV DNA in plucked eyebrow hair has been well investigated (Boxman et al., 1997) in renal transplant recipients and immunocompetent patients (ICPs) and correlated with both benign and malignant cutaneous lesions (Struijk et al., 2003; Plasmeijer et al., 2009), very little is known about HPV prevalence in eyebrow hair from HIV patients.

The study design was approved by the research ethics committee and all

Abbreviations: HPV, human papillomavirus; ICP, immunocompetent patient

Three-base deletion mutation c.120_122delGTT in *ATP2A2* leads to the unique phenotype of comedonal Darier disease

D. Tsuruta, M. Akiyama,* A. Ishida-Yamamoto,† H. Imanishi, N. Mizuno, J. Sowa, H. Kobayashi, M. Ishii, I. Kurokawa‡ and H. Shimizu*

Department of Dermatology, Osaka City University Graduate School of Medicine, Osaka, Japan
*Department of Dermatology, Hokkaido University Graduate School of Medicine, Sapporo, Japan
†Department of Dermatology, Asahikawa Medical College, Asahikawa, Japan
‡Department of Dermatology, Mie University Graduate School of Medicine, Tsu, Japan

Darier disease (DD; Darier–White disease; OMIM 124200) is an autosomal dominant inherited disorder.[1] Clinically, it is characterized by recurrent and multiple hyperkeratotic papules or nodules affecting the trunk and flexural aspects of the extremities.[1] Characteristic histopathological features are dyskeratotic cells in the form of corps ronds and grains, suprabasal acantholysis forming suprabasal lacunae and irregular upward proliferation into the lacunae of papillae lined with a single layer of basal cells, the so-called villi.[2] The causative gene is *ATP2A2* (OMIM 108740) on chromosome 12, which encodes the sarco/endoplasmic reticulum calcium pump ATPase (SERCA2).[2]

Clinical variants include the hypertrophic, vesiculobullous, hypopigmented, cornifying, zosteriform and linear subtypes, and the rare subtype comedonal Darier disease (CDD).[1,3–6] CDD tends to appear in seborrhoeic areas. The characteristic morphological features are prominent follicular involvement, sometimes associated with keratotic plugs, and the presence of greatly elongated dermal villi and papillary projections.[4] There have been no conclusive reports on the aetiology of CDD and it is still controversial as to whether or not CDD is a variant of DD, and if it is caused by *ATP2A2* gene mutations, although a combination of CDD and classic DD was reported in one patient.[7] The present study identifies a previously unreported three-base deletion mutation in *ATP2A2* in a patient with CDD.

Patient and methods

A 22-year-old Japanese man presented with acne-like comedonal lesions on the face and chest, most densely distributed on the forehead, cheeks, back, axillae and chest. The comedonal lesions had first appeared in his teens and had gradually increased in number. Physical examination showed open comedones, closed comedones, red papules, nodules, cysts and ice-pick scars (Fig. 1a,b). His parents were clinically healthy, without any skin problems. He had been treated with oral biotin, Korean ginseng, an antihistamine, topical bufexamac ointment, calcipotriol ointment and betamethasone butyrate propionate ointment without any improvement. Histopathological observations revealed suprabasal acantholytic clefts and numerous dyskeratotic cells (corps ronds) in the outer root sheath in the affected follicular infundibulum, which was surrounded by plasma cells and lymphocytes (Fig. 1c,d). We made a diagnosis of CDD. Oral etretinate 10 mg daily combined with adapalene gel remarkably improved most of the skin lesions, except those on the forehead.

Polymerase chain reaction (PCR) amplification and direct sequencing of the entire coding region and exon/intron boundaries of *ATP2A2* were performed using the proband's and his parents' genomic DNA samples and genomic DNA samples from 50 healthy Japanese individuals as controls. A detected mutation was verified by mutant allele-specific amplification analysis[8] with mutant allele-specific primers carrying the substitution of two bases at the 3′ end, a PCR product band derived from the mutant allele.

This study was approved by the Hokkaido University Medical Ethics Committee and conducted according to the principles of the Declaration of Helsinki. All clinical samples were obtained with informed consent.

Results and discussion

Direct sequencing of *ATP2A2* in the proband's genomic DNA revealed a heterozygous three-base deletion c.120_122delGTT in exon 2, which causes deletion of leucine at the 41st amino acid residue from the amino terminus (p.Leu41del). This mutation was not detected in his parents nor in 100 normal unrelated alleles from 50 healthy individuals (Fig. 2). No other pathogenic mutations were detected within *ATP2A2* in the patient's DNA. By mutant allele-specific amplification ana-
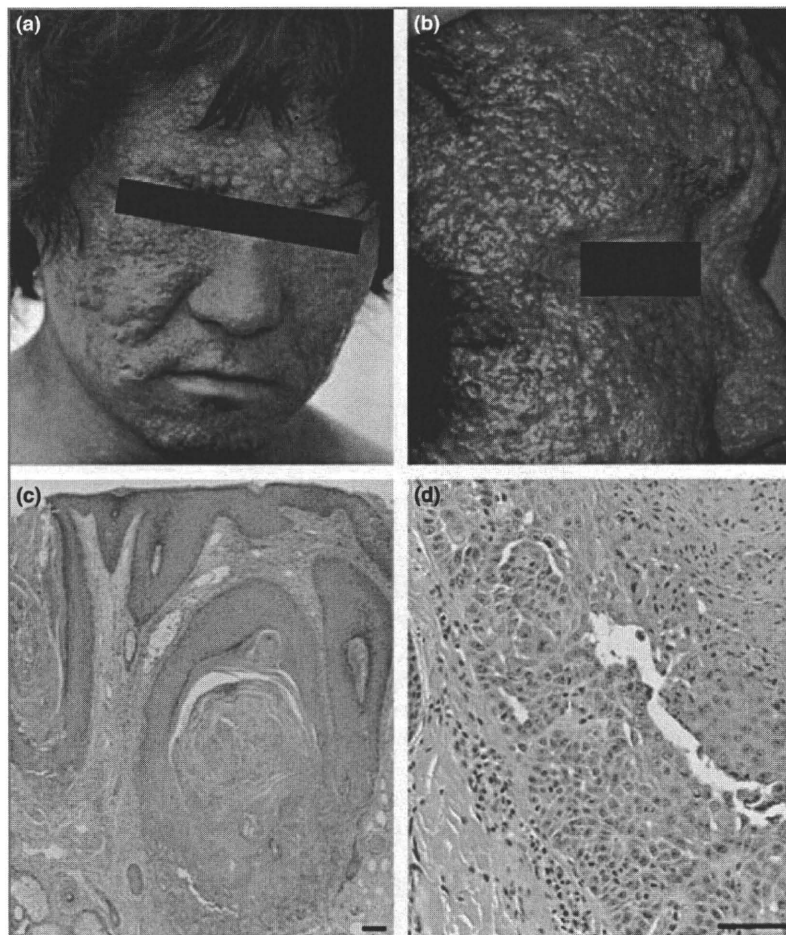
Fig 1. Unique clinical and histological features of comedonal Darier disease in the patient. (a, b) Open comedones, closed comedones, red papules, nodules, cysts and ice-pick scars are present on the face. (c, d) Histology of the comedonal lesions. Dilated, cystic hair follicles with keratin plugs are seen in the dermis (c). Suprabasal acantholytic clefts and numerous dyskeratotic cells in the form of corps ronds are apparent in the outer root sheath in the affected follicular infundibulum (d). Bars = 100 mm.

lysis,[8] a PCR product band derived from the mutant allele was amplified from the patient's genomic DNA, but not from either parent nor from the control DNA samples.

Since the first description of CDD by Derrick *et al.*,[4] only seven cases including the present one have been reported. The present case is the first in which a causative mutation has been identified. *ATP2A2* gene mutations in DD have been reported to result in alterations in calcium signalling during keratinocyte differentiation, causing acantholytic dyskeratosis.[2,9,10] The function of SERCA2 is to pump calcium from the cytosol to the endoplasmic reticulum and to excite oscillation of calcium spikes in the cytosol.[11–13] The mutation site in our patient localized to the first stalk (S1) of SERCA 2. The S1 region adjacent to transmembrane helices is considered to be highly conserved at the amino acid level by many species.[2] p.Leu41-del in S1 of SERCA2 is considered to impair calcium-binding sites in the α-helix of the region that contains a signal for sarco/endoplasmic reticulum localization, and to change the conserved alignment of five glutamic acid residues.[11,14] Several mutations in the S1 region of *ATP2A2* in DD have been reported.[2,10,14–16] In addition, the dephosphorylation process of SERCA2 is thought to be important for Ca^{2+} ion release into the lumen by SERCA2 and, recently, Miyauchi *et al.*[17] reported that both p.Leu41del and p.Pro42del mutations

inhibit the dephosphorylation process. The present c.120_122delGTT mutation has not been reported, although a heterozygous deletion of the identical leucine residue, c.121_123delTTA (p.Leu41del), was reported in one patient.[14] The patient showed severe hypertrophic scar formation in addition to common DD skin manifestations and had severe emotional problems and a family history of suicide.[14] Our patient with CDD had a quite different skin phenotype and showed no mental problems. We do not know exactly why the phenotype differs between our case and the previously reported cases. There is a possibility that a silent mutation or allelic variant of *ATP2A2* may have affected the phenotypic expression in our patient and/or the previously reported cases. Certain environmental factors, such as mechanical trauma, sun exposure, heat and sweating often define a phenotype of DD,[2] and such factors may be related to the formation of the CDD phenotype in our patient, because the face is more frequently affected than other body sites by environmental factors. Further functional studies are required to elucidate the pathomechanisms of CDD, a unique phenotype of DD. Interestingly, an *ATP2A2* mutation was reported to underlie two cases from one British family with another unique phenotype, acrokeratosis verruciformis (AKV), providing evidence that AKV and DD are allelic disorders.[18] On the other